1-1-2010

Analysis of the Effect of Various Ligands on the Hydrolysis of Ruthenium (III) Complexes and Interpretation of Kinetics of Hydrolysis Profiles by UV-Visible Spectrophotometry

Sudheer Koneru

Analysis of the Effect of Various Ligands on the Hydrolysis of Ruthenium (III) Complexes and Interpretation of Kinetics of Hydrolysis Profiles by UV-Visible Spectrophotometry

by

Sudheer Koneru

Thesis

Submitted to the Department of Chemistry

Eastern Michigan University

In partial fulfillment of requirements

for the degree of

MASTER OF SCIENCE

in

Chemistry

December 2010

Ypsilanti, Michigan.

DEDICATION

TO

My Family,

Friends and

Chemistry Department, EMU.

ACKNOWLEDGEMENTS

I would like to thank my research advisor, Dr. Timothy Brewer. His interest, knowledge, guidance, encouragement, and patience helped me in successful completion of this project.

I am greatly thankful to Dr. Larry Kolopajlo and Dr. Jose Vites for agreeing to serve on my thesis committee.

I would like to thank my graduate advisor, Dr. Timothy Brewer, for his excellent support by awarding me a graduate assistantship and for his valuable academic suggestions throughout my Master's in chemistry department.

I would like to thank the head of the chemistry department, Dr. Ross Nord, all professors, staff, and all my friends at EMU chemistry department, who helped me during my Master's in Eastern Michigan University.

Finally, I would like to thank my parents and my brothers, who gave moral support throughout my Master's degree at Eastern Michigan University.

ABSTRACT

Cancer is one of the major causes of death in the world. Discovery of platinum metal-based drugs like cisplatin and carboplatin have proved to be successful in cancer treatment. Due to subsequent development of resistance, side effects, and fewer toxic effects of these drugs, the usage of these drugs has been limited. Novel drugs were being synthesized utilizing the transition metals like ruthenium, osmium, and copper.

In this research, ruthenium metal complexes of the formula $HL[RuCl_4L_2]$ (where L= ligand) were synthesized. These ruthenium-based drugs exist in prodrug forms which are activated into antitumor drugs by means of hydrolysis, redox reactions, or reactions with biological nucleophiles. In these reactions, ruthenium is reduced to the active Ru(II) form from its inactive Ru(III) state. In this research work, three ruthenium complexes with different ligands of varying basicity are synthesized, and their hydrolysis reactions are studied under different pH values using UV-Visible spectrophotometry at room temperature. The ligands utilized in this project are imidazole, thiazole, and 1H-1,2,4-triazole. Among these, ruthenium imidazole has passed the Phase I clinical trials. For the ruthenium-imidazole (RIM) complex and the ruthenium-thiazole (RTZ) complex, rates of the hydrolysis reaction are determined by fitting the experimental data to proposed kinetic models for these complexes. The kinetic models proposed did not help in the determination of the rate of hydrolysis of the ruthenium-triazole (RTrz) complex as the absorbance trend of the RTrz complex in acidic pH values was opposite to the trend displayed by the RIM and RTZ complexes indicating a different hydrolysis mechanism for the RTrz complex.

The comparative data will aid in better drug design and evaluation of pharmacokinetic parameters. Future studies on hydrolysis of these complexes at different pH values using HPLC and NMR spectroscopy might reveal the exact mechanism and may lead to characterizing the products formed in the hydrolysis process.

TABLE OF CONTENTS

LIST OF TABLES

Table

LIST OF FIGURES

Figure

CHAPTER 1: INTRODUCTION

Metal-based drugs are the primary choice among the various drugs available for the chemotherapy of cancer. A platinum-based drug called cisplatin was the most widely used drug for treatment of ovarian, testicular, neuronal, and other tumors. The success of cisplatin increased the interest of many scientists to develop more metal-based anti-tumor drugs. Progress in this field has led to different kinds of ruthenium complexes being synthesized and studied. Ruthenium reduces the disadvantages associated with cisplatin such as toxicity and drug resistance.[1] Compounds like ruthenium imidazole (RIM) and ruthenium indazole (RIN) are already in Phase I clinical trials and they proved to be successful anticancer drugs.[2,3] As a further investigation, we synthesized and analyzed the hydrolysis rate of ruthenium complexes with different ligands like imidazole, thiazole and 1H-1,2,4-triazole.

The different complexes of ruthenium were analyzed for their hydrolysis profiles under different pH conditions from pH 4.0 to 9.0 at room temperature. Proposed mechanisms and interpretation of the kinetics based on the ligand properties are presented.

1.1 Cancer

Abnormal growth of cells due to uncontrolled division of the cells at intractable rates and the ability of these cells to invade and damage normal tissues of the body is known as cancer. These cancerous cells can spread throughout the body, and this spreading occurs through blood and lymph systems. The main cause of this abnormal growth of cells is the damage of DNA through various genetic factors or environmental mutagens. Based upon the ability of the tumor to spread to other parts of the body, tumors may be classified as benign and malignant. Of these two, malignant tumors are actually classified as cancerous growth.[4,5,6]

Benign tumor: These tumors are localized and do not undergo metastasis. They are not harmful to the body because they do not spread to the surrounding organs or tissues. They can be easily removed by simple surgery.[4,5]

Malignant tumor: These tumors actually come under the category of cancerous tumors. They undergo rapid metastasis and spread the cancer to surrounding tissues and organs, resulting in abnormal growth of the cells. This type of tumor requires aggressive therapy involving surgery, radioactive therapy, or chemotherapy, or in some cases a combination of these therapies is required.[6]

1.1.1 Types of Cancer

Cancer is classified into several types, and they are named based upon the place of origin of the cancerous growth.[5,7] The following illustrates some of these classifications and their origin:

Carcinoma: In epithelial cells of skin, digestive tract, glands, and so on.

Leukemia: In the stem cells of bone marrow tissue.

Lymphoma: In lymphatic tissue.

Melanoma: In melanocytes.

Sarcoma: In connective tissues of bone or muscle.

Teratoma: In germ cells.

1.1.2 Treatment of Cancer

The treatment of cancer may be done by a single method or a combination of methods. The treatment mainly depends upon the type and location of the cancer. If the disease has spread to other parts of body, a combination of the following methods is more effective.[5,6]

Surgery is one of the cancer treatment methods that remove cancer. This is the most common way to treat cancer. It is very rare that the cancer will spread during the surgery.

Radiotherapy is a treatment that uses high energy radiation to kill cancer cells in the affected area. The advantage of this treatment method is that it is relatively painless.

Chemotherapy is a method of killing cancer cells using drugs. However, it may also harm the healthy cells. The body will start to produce normal cells after the chemotherapy is over.

Hormone therapy is a method that uses an antagonist to prevent the production of other hormones needed for cancer cell growth or uses drugs to stop the production of some hormones. In some cases it might require removal of the hormone-producing organ to prevent secretion.

Side effects of these treatments include terrible pain, nausea, temporary fatigue, and vomiting.

1.1.3 Drugs Available for Treatment of Cancer

The anticancer drugs can be classified into various types based upon their chemical structure or based upon their biochemical mechanism. Alkylating agents and antimetabolites are the drugs most widely used to treat different forms of cancer. The metal-based drugs, mainly the

platinum complexes, especially cisplatin, which are classified under the alkylating agents, are often used as the first line of treatment in testicular and ovarian cancers. These drugs bind to DNA and form adducts which block the synthesis of DNA and RNA, thereby inducing cell death. Side effects like nephrotoxicity, neurotoxicity, ototoxicity, alopecia, and development of resistance restricts the usage of the platinum complexes.[6,8,9,10]

1.1.4 Molecular Mechanism of Action of Antitumor Drugs

Cisplatin is the most widely used drug for treating metastatic testicular and ovarian tumors. The three main components involved in the antitumor activity by metal-based drugs include the metal-based drug, DNA, and HMG-protein.[11]

The drug cisplatin is mainly transported into the cancer cell through active transport. Sometimes it may occur through passive transport. After entering into the cell, cisplatin forms adducts with two consecutive guanine bases of DNA. The chloride ions of cisplatin are displaced by the nitrogen bases of DNA. This is due to the greater affinity of cisplatin for nitrogen bases compared to its affinity for chlorine. Adduct-induced DNA bending allows the binding of proteins with the highly mobile HMG domain. Once protein is bound to DNA, it inserts a wedge like phenyl group of phenylalanine into the adduct. The tightly bound HMG protein causes the destacking of nucleotide bases, resulting in the inactivation of the DNA helix. With the HMG protein bound to DNA, the modified strand cannot be repaired and hence the cell dies.[11]

1.2 Ruthenium

Ruthenium can be considered to be a good alternative to platinum because of its wide range of oxidation states that are accessible under normal physiological conditions. The activity

of many anticancer drugs is dependent upon their oxidation states, and hence ruthenium is an excellent choice. The synthetic versatility, ability to change ligand affinities, high selectivity, and ability to mimic iron in binding to various biomolecules make ruthenium a viable alternative in anticancer drug development studies. The first ruthenium compound to be tested for its antitumor activity, ruthenium imidazole, was developed by M. Clarke.[12]

Ruthenium exists in two forms; one is the inactive Ru(III) form and the other is the active, reduced Ru(II) form. Generally ruthenium complexes tend to remain in the Ru(III) inactive form. Upon reaching the tumor site, ruthenium is reduced to the potent and active Ru(II) state, which is selectively toxic to tumor cells. This reduction is favored by the environment surrounding the cancer cell which has a lower pH and low oxygen content than the healthy tissue.[1,12] Like platinum complexes, ruthenium complexes exhibit antitumor effects, inhibiting the synthesis of DNA and RNA, by forming DNA adducts.[13,14]

1.2.1 Ruthenium Complexes Used in this Study

The compounds used for this study were imidazolium *trans*-bis(imidazole) tetrachlororuthenate (III) {HIm[*trans*-$RuCl_4(im)_2$]} (RIM), which has passed the Phase I clinical trials; thiazolium *trans*-bis(thiazole) tetrachlororuthenate (III) {HTz[*trans*-$RuCl_4(Tz)_2$]}(RTZ); and 1H-1,2,4-triazolium *trans*-bis(triazole) tetrachlororuthenate (III) {HTrz[*trans*-$RuCl_4(Trz)_2$]} (RTrz). These compounds are shown in Figures 1 through 3.

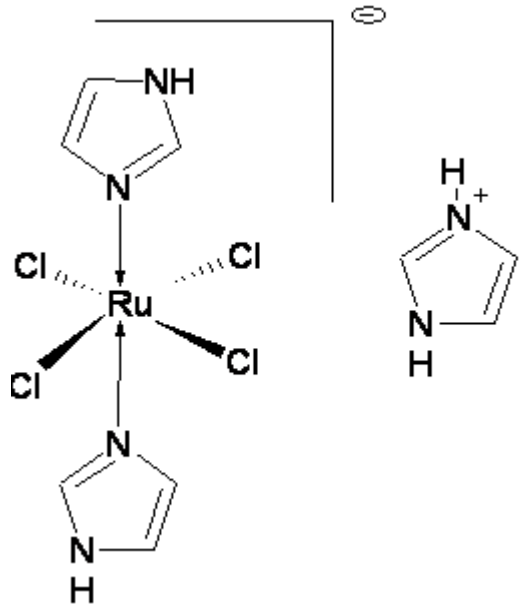

Figure 1. Chemical structure of HIm [*trans*-$RuCl_4(Im)_2$]

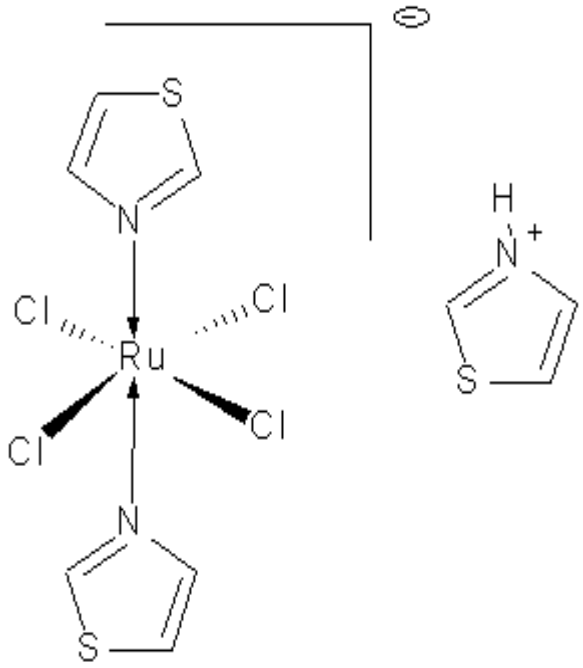

Figure 2. Chemical structure of HTz [*trans*-$RuCl_4(Tz)_2$]

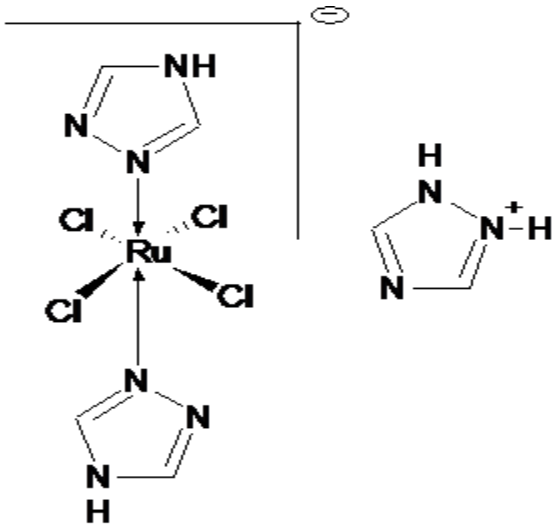

Figure 3. Chemical structure of HTrz [*trans*-$RuCl_4(Trz)_2$]

1.3 Hydrolysis

The mechanism of this hydrolysis reaction involves the displacement of a ligand by a molecule of water. This ligand displacement is important because ruthenium complexes become activated by this process.

1.4 Kinetics of Hydrolysis and its Importance in Cancer Studies

The study of the rates of chemical reactions is called kinetics. The kinetics can be studied in various ways including changing various conditions such as concentration and pH. The metal-containing antitumor drugs are usually in their inactive prodrug form and they become reduced to their active form by means of hydrolysis. The time taken for the conversion of a prodrug into an active drug is important in cancer studies because it determines the onset of action, duration of action, and the clearance rate of drugs.[7,15] These kinetic studies will aid in the development of drugs with enhanced stability, increased potency, and activity.

Ruthenium complexes exist in prodrug form, before they are injected into the body. They are activated into the active Ru(II) form by changing their coordination. Then they react with the biomolecules and exert their therapeutic activity. This activation can be achieved through various reactions, such as hydrolysis, involving formation of aqua complexes, ligand substitution, and redox processes.[1,7,15] Hydrolysis is important, as proven with cisplatin, because the prodrug is activated by means of formation of aqua complexes through hydrolysis. Aqua complexes are orders of magnitude more labile than chloro complexes resulting in more active compounds.[7,15]

The ruthenium (III) complexes of the general formula $HL[RuCl_4L_2]$, contain two *trans* bonding heterocyclic ligands L bound to ruthenium via nitrogen. The possible mechanism of hydrolysis of ruthenium complex bound with heterocyclic ligands is shown in Figure 4. Initially one or two chloride ions are substituted with water molecules, and then the resulting ruthenium complexes bind to each other, forming polynuclear complexes. These polynuclear complexes bind to DNA, forming adducts, and thereby exert their antitumor activity.[16]

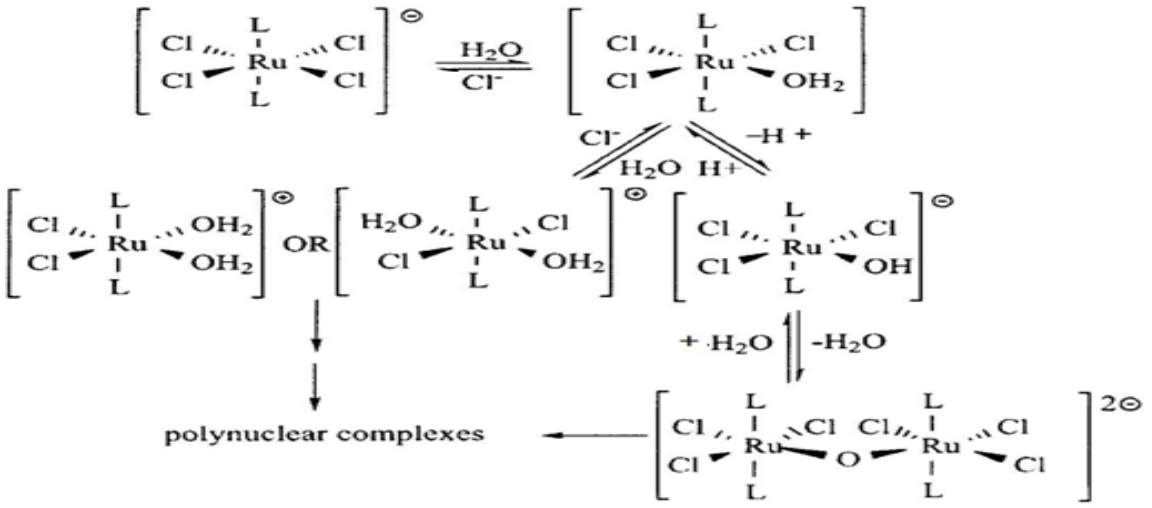

Figure 4. Possible mechanism of hydrolysis of ruthenium complex anion trans-$[RuCl_4L_2]$
*(Figure from J. of Inorg. Biochem. **2004**, 98, 402-412).*[17]

Bouma *et al.* suggested two possible transformations of NAMI-A, imidazolium *trans*-tetrachloro (dimethylsulfoxide) imidazoleruthenium (III) {H_2Im [*trans*-$RuCl_4$(DMSO-S)HIm]}, a ruthenium complex, in Phase I clinical trials of a cancer study. Initial transformation includes the ligand substitution, which depends upon the buffer pH and further transformation including the substitution of ligands or reduction of Ru(III). In acidic media of pH less than 6, the decomposition of NAMI-A follows pseudo first order kinetics. At pH values greater than or equal to 6, it follows zero order kinetics. The complex tends to be most stable at a pH of 3-4.[16, 17]

Velders *et al.* in search of new ruthenium (III) complexes having a better pharmacological profile, synthesized the pyrazole, thiazole, and pyrazine analogues of NAMI-A. These compounds showed a better onset of action than the NAMI-A.[18]

Mura *et al.* studied the stability and hydrolysis of thiazolium *trans*-tetrachlorobis (thiazole) ruthenate (III) complex in different solvents at different pH values. In previous studies of NAMI-A with the less basic ligand-thiazole, a significant decrease in the rate of chlorine exchange with water molecules was observed. The increase in half life of the hydrolysis, compared to NAMI-A, indicates the stabilizing influence of thiazole on the hydrolysis of ruthenium (III) complex due to replacement of imidazole with the less basic thiazole ligand.[19]

Messori *et al.* conducted studies on hydrolysis of another ruthenium (III) complex, aminothiazolium *trans*-tetrachlorobis (aminothiazole) ruthenate (III), in different solvents of varying pH values.[20] Upon comparing different nitrogen-based ligands, these studies indicate that the more basic the heterocyclic ligand of the ruthenium complex is, the higher the rate of hydrolysis. The higher electron transfer from the nitrogen to the metal in the ruthenium complex increases the dechlorination rate by weakening the metal–chloride bond.[7,21,22]

Keppler *et al.* analyzed the ruthenium (III) complex, 1H-1,2,4-triazole [*trans*-tetrachloro ruthenate(III) triazole(DMSO)] for the rate of dechlorination and compared it with RIM and RIN complexes. Studies proved that the greater electron donor character of neutral ligands and the basicity of azole ligand will promote solvolytic dechlorination, which in turn reduces Ru(III) to Ru(II).[22] In my present research, nitrogen-based ligands of varying basicity were used, and an attempt was made to determine the effect of basicity of these ligands on the hydrolysis of the ruthenium (III) complexes, which might support or oppose the theory proposed by Keppler *et al.*

Based upon the studies conducted by different researchers, ruthenium complexes with enhanced activity and potency can be developed. According to Messori *et al.* hydrolysis of the thiazole complex was found to be fastest when the compound was dissolved in a buffer of pH 7.4 compared to other pH levels.[19] Arion *et al.* proved that decreasing the basicity of ligand significantly reduces the reduction rate of Ru(III) to Ru(II), thereby limiting the accessibility of the ligand to interact with the tissues. This process does not allow hydrolysis until the drug reaches its final target.[18,22]

1.5 Research Goal

The main theme of this research was to study the effect of various ligands (L=imidazole, thiazole, 1H-1,2,4-triazole) on the hydrolysis of the ruthenium(III) complexes of general formula HL[*trans*-$RuCl_4L_2$] at room temperature in buffers of varying pH values. This study will allow a comparison of the kinetics of the RIM complex, which already passed the Phase I clinical trials, with the other ligands by determining their respective rate constants of hydrolysis reaction.

CHAPTER 2: EXPERIMENTAL PROCEDURES

2.1 Instrumentation

A Perkin Elmer Lambda-25 Ultraviolet-Visible spectrophotometer was coupled with a Perkin Elmer temperature controller to analyze the kinetics of the hydrolysis of ruthenium compounds. The pH of buffer solutions was measured using a Hanna 8417 pH meter.

2.1.1 UV-Visible Spectrophotometer

The ultraviolet-visible (UV-Vis) spectrophotometer is an instrument that analyzes the absorbance of compounds in the ultraviolet and visible regions of the electromagnetic spectrum. Unlike infrared spectroscopy which detects vibrational motions of molecules, ultraviolet-visible spectroscopy detects electronic transitions. The basic principle in analyzing the absorbance by UV-Vis spectrophotometer is the Beer-Lambert law. This law states that the absorbance of a solution is directly proportional to the concentration of solution:

$$A = € b c$$

where,

A = absorbance of the solution

€ = molar absorptivity coefficient

c = concentration

b = path length

In general, a hydrogen or deuterium lamp is the light source for the ultraviolet region from 250-400 nm, and a tungsten or halogen lamp is the light source for the visible region of 400-800 nm. The solvent and sample solutions are placed in the reference and sample cells, respectively. Monochromatic light from the source is allowed to pass through the cells, and the

transmitted light is measured by a detector.[23] The basic design of a UV-Vis spectrophotometer is illustrated in Figure 5.

Ultraviolet and visible light are energetic enough to promote valence electrons to higher energy levels. UV-Vis spectroscopy is usually used for inorganic ions or complexes in solution because of their strong absorptions. The UV-Vis spectra have broad features that do not limit their use only for sample identification but are also very useful for quantitative measurements.

The electronic transitions that are detected by the UV-Visible spectrometer result in absorption maxima in the spectra, which occur due to the excitation of valence electrons of a compound from the ground level to higher energy levels. In other words, it can be described as the excitation of electrons from bonding and nonbonding orbitals to the antibonding or nonbonding orbitals.[23]

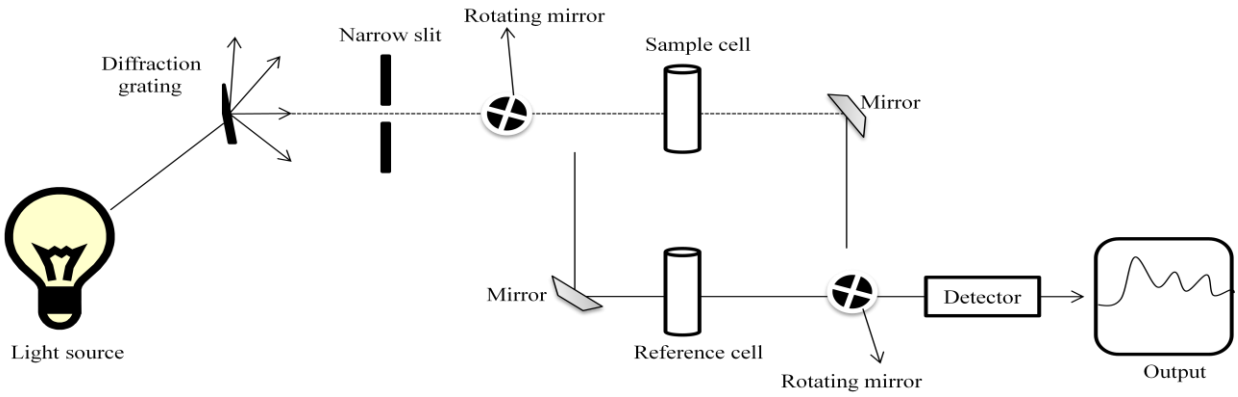

Figure 5. Schematic representation of UV-Visible spectrophotometer.

2.2 Materials

Ruthenium (III) chloride hydrate (Reagent plus, Sigma Aldrich), imidazole (99%, Aldrich), thiazole (96% Aldrich), 1H-1,2,4-triazole (97% Aldrich) were used as purchased for the preparation of ruthenium complexes. Monosodium phosphate hydrate ($NaH_2PO_4.H_2O$)

(Analytical reagent, Mallinckrodt), disodium phosphate hydrate ($Na_2HPO_4.H_20$), citric acid ($C_6H_8O_7$) and sodium chloride (NaCl) (Certified A.C.S, Fischer) were used for the preparation of buffers.

Synthesis:

Synthesis of HIm[*trans*-$RuCl_4(Im)_2$]: In a mixture of 25.00 ml of ethanol and 25.00 ml of 1.00 N HCl, 1.00 gram of $RuCl_3$ was dissolved. This mixture was refluxed for three hours, and the resulting solution was evaporated to 9.00 mL. The final volume of the solution was made to be 12.00 mL with 1.00 N HCl. Next, a suspension is prepared by adding 2.00 grams of imidazole to 1.00 mL of 6.00 N HCl, into which 10.00 mL of the ruthenium solution prepared above was added. Then the solution was cooled in ice for two hours and allowed to stand for two days at room temperature. The large brownish red crystals formed were filtered off and washed with 1:1 water and ethanol mixture to remove impurities, and dried under vacuum.[22,24]

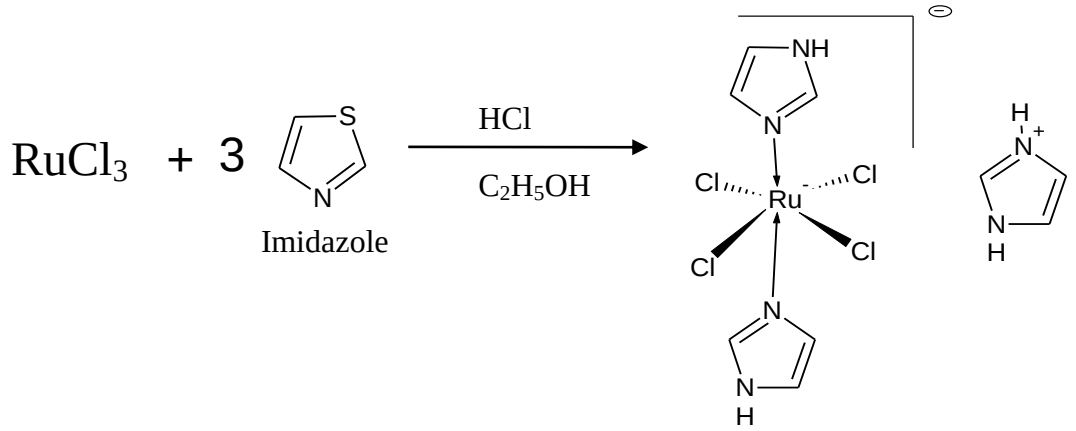

Figure 6. Synthesis of Ruthenium-Imidazole Complex.

Synthesis of HTz[*trans*-$RuCl_4(Tz)_2$]: 1.00 grams of Ruthenium chloride was dissolved in 10.00 mL of ethanol and 10.00 mL of 1.00 N HCl and refluxed gently for 90 minutes. A solution of 1.92 grams of thiazole dissolved in 2.00 mL of ethanol and 2.00 ml of 6.00 N HCl was added to

the ruthenium solution with continuous stirring. The solution was refluxed gently for 30 minutes, forming a precipitate. Then the brownish red microcrystals were separated by filtration, washed with ethanol and ether, and dried under vacuum.[19]

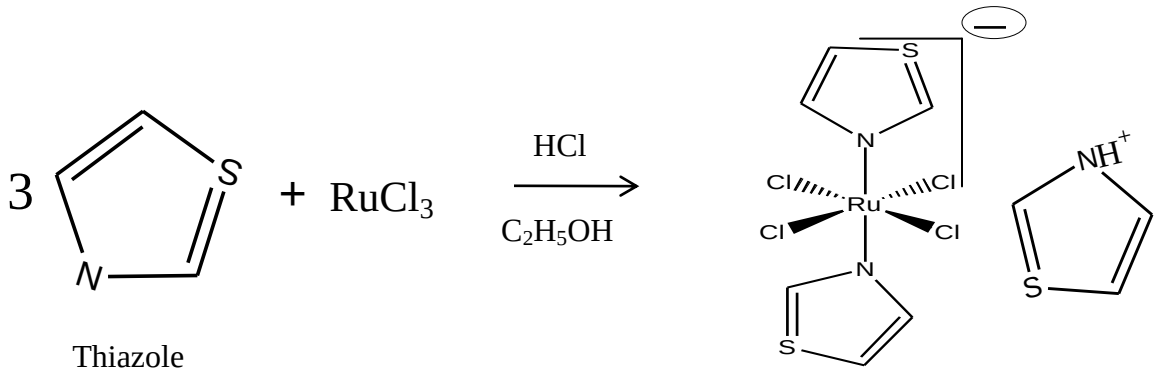

Thiazole

Figure 7. Synthesis of Ruthenium-Thiazole Complex.

Synthesis of HTrz[*trans*-$RuCl_4(Trz)_2$]: 1.00 grams of ruthenium chloride was added to 2.00 grams of 1H-1,2,4-triazole and refluxed for about two hours. The solution was filtered to obtain large orange crystals of ruthenium triazole complex. The isolated crystals were washed initially with ethanol and later with diethyl ether to remove the impurities and finally dried under vacuum.[22,26]

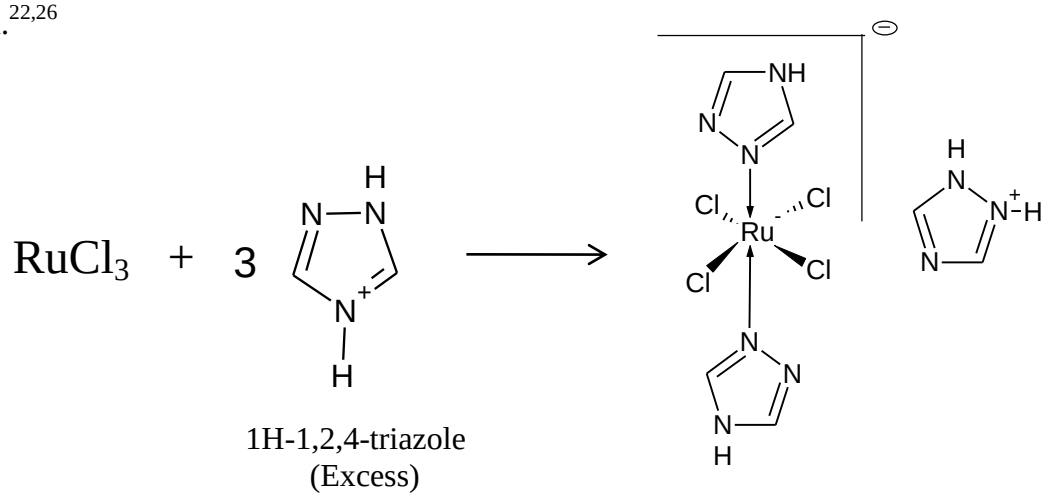

1H-1,2,4-triazole
(Excess)

Figure 8. Synthesis of Ruthenium-Triazole Complex.

Phosphate buffers: Buffers of pH 4.0, 5.0, 6.0, 7.5, and 9.0 were prepared by using appropriate volumes of 50 mM monosodium phosphate and 50 mM disodium phosphate and 100 mM sodium chloride in distilled water. Small amounts of 10% citric acid and 10% sodium hydroxide solutions were used to adjust the pH of each buffer to the desired value.

2.3 Hydrolysis Kinetics Study

All complexes were found to be significantly soluble in water, making a comparative kinetic study possible. The complexes were dissolved in freshly prepared buffers, and their absorbances were recorded over time using the Perkin Elmer Lambda 25 UV-Vis spectrophotometer. During analysis of the complexes in various pH solutions, the initial concentration of the complexes was kept constant. For example, in all buffer systems of pH values 4.0 to 9.0, the concentration of RIM complex was initially 0.050 M. This enables a comparison of the data due to similar initial concentration of the complex throughout the analysis.

The following steps were followed in preparation of the sample and analysis of hydrolysis of the RIM complex:

1. 2.25 grams of RIM complex were weighed into a 150 mL beaker.
2. 100 mL of water containing phosphate buffer was added to dissolve the RIM complex.
3. The solution was mixed for approximately one to three minutes until a clear and light red-colored solution was obtained.
4. The solution was transferred to a sample cuvette and the reference cuvette was filled with blank solution containing phosphate buffer of the corresponding pH being investigated.

5. Then the kinetic analysis was initiated. The pH of the mixture was recorded before initiation of the analysis. The spectrophotometer was connected to a temperature bath to maintain a temperature of $25^{o}C \pm 1^{o}C$. There was a delay of approximately 2-3 minutes between mixing and initiation of the kinetic run. The absorbance was recorded at a determined wavelength for approximately six hours, and the final absorbance was measured after a day to allow the reaction to reach completion.
6. At end of reaction, the pH of the reaction mixture was recorded.

The pH meter was calibrated using standard buffer solutions of pH 7.0 and 4.0 containing monobasic sodium phosphate and dibasic sodium phosphate. During these studies, the ratio of masses of ruthenium complex and water was generally maintained around 1:100. The initial concentration of the complexes was maintained constant in all buffer solutions (0.050 M for RIM, 0.045 M for RTZ, and 0.010 M for RTrz) during the kinetic runs.

The solutions of RIM and RTZ complexes were clear when initially prepared, but they gradually become turbid over time during analysis. This turbidity may be due to a precipitation reaction. Due to the gradual precipitation, these solutions exhibited increasing absorbance over time.

In acidic pH, the solution of RTrz complex was hazy during the initiation of kinetic run. But the solution became clear during the analysis. The RTrz complex solution in basic pH was initially clear but became turbid over time. The turbidity in the solutions of all the complexes was anticipated due to the precipitation occurring in solution. Both the solution and precipitate were analyzed using NMR spectrometry, but the paramagnetic nature of ruthenium made it difficult to characterize the product being formed.

It should be noted that there might be certain inconsistencies occurring in the initial absorbance readings and the concentrations based upon factors including mixing time needed for a given complex to dissolve in the solution of a particular pH and the time delay between the actual dissolution of the complex and initiation of the kinetic study. The reaction for a given pH buffer was run several times and the best two or three trials were used to determined the average rate constant.

Absorbances were analyzed over a wavelength range of 300-700 nm. Wavelengths selected for studying the kinetics of the hydrolysis reaction were based upon maximal changes in absorbance of hydrolyzed complexes. The wavelengths used are 340 nm for RIM, 365 nm for RTZ, and 360 nm for RTrz. Hydrolysis studies were done at pH values of 4.0, 5.0, 6.0, 7.5, and 9.0. All reactions were studied at room temperature, $25^{o}C \pm 1^{o}C$. Analysis of data for the kinetic studies was performed using the Graphical Analysis program from the Vernier software data analysis package.

CHAPTER 3: RESULTS and DISCUSSION

3.1 Mechanism of Kinetics of Hydrolysis of Ruthenium Complexes

The general mechanism of the hydrolysis of ruthenium complexes is proposed to involve two steps, the formation of intermediate from the reactant and the formation of the final product from the intermediate. The theory behind the calculation of the kinetic equation to describe this process involves the classical Arrhenius theory. The two steps of hydrolysis of ruthenium complexes can be shown as follows:

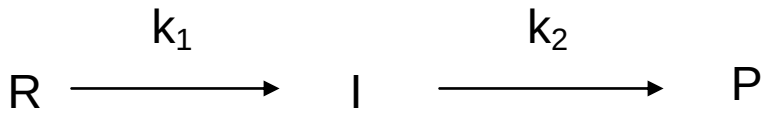

As shown in the above reaction, the hydrolysis of ruthenium complexes is proposed to follow a two-step reaction. The reactant (R) converts into an intermediate (I), the substituted complex with water molecules or hydroxide ions. The second step involves the formation of final product (P), polynuclear complexes formed due to the combination of substituted ruthenium complexes. The rate constants of the two steps are denoted as k_1 and k_2, respectively.

The kinetics for this mechanism can be modeled by solving the differential equations involving the concentrations of the reactant [R] , intermediate [I], final product [P] and initial concentration of reactant $[R]_0$ by equations shown below:[7,27]

$$[R] = [R]_0 \, e^{-k_1 t} \qquad (1)$$

$$[I] = (k_1 [R]_0 / (k_2 - k_1)) * (e^{-k_1 t} - e^{-k_2 t}) \qquad (2)$$

$$[P] = [R]_0 - [R] - [I] = [R]_0 * \{1+[(1/(k_1-k_2)) * (k_2e^{-k_1t} - k_1e^{-k_2t})]\} \quad (3)$$

In all of the equations (1), (2), and (3), the concentrations of reactant, intermediate, and product are functions of time. These equations were used to determine the rate constants. Beer's law relates concentration to absorbances in order to determine the kinetic rate constants for these models.

3.2 RIM and RTZ Complexes

As stated previously, the hydrolysis follows a two-step reaction. The formation of an intermediate (I) from the reactant (R) is the first step, followed by the formation of product (P) from the intermediate as the second step. The respective rate constants for the first and second steps are denoted by k_1 and k_2, respectively.

In both of these complexes, an induction period was observed in the absorbance spectrum at all acidic pH levels. This induction period was assumed to be due to the formation of intermediate. The induction period was found to decrease as the pH is increased. At basic pH levels, this period was reduced to less than 20 minutes, indicating that higher pH levels caused a faster formation of the intermediate.

Utilizing absorbance of the complexes instead of concentrations in equations (1) to (3), the rate constants of the two steps can be calculated as discussed below. The absorbance for each species is given by the equations (4) – (6), which were derived from solving the proper differential equations.

$$Abs_R = A\ e^{-k_1 t} \quad (4)$$

$$Abs_I = C\,(k_1/\,(k_2-k_1))\,(e^{-k_1t} - e^{-k_2t}) \quad (5)$$

$$Abs_P = E\,(1 + 1/(k_1 - k_2))\,(k_2e^{-k_1t} - k_1e^{-k_2t}) \quad (6)$$

The total absorbance (Abs_T) is obtained by summing the absorbance of the reactant (Abs_R), intermediate (Abs_I), and product (Abs_P). These absorbances can be related to the rate constant (k_1) of the first step as given in equation (7).

$$Abs_T = Abs_R + Abs_I + Abs_P$$

$$Abs_T = Ae^{-k_1t} + C\,(k_1 / k_2-k_1)\,(e^{-k_1t} - e^{-k_2t}) + E\,(1+ (1/k_1-k_2)\,(k_2e^{-k_1t} - k_1e^{-k_2t})) \quad (7)$$

The constants A, C, and E are related to the initial concentration of reactant and the molar absorptivities of the reactant, intermediate, and product, respectively. The term k_1 is the rate constant of the first step of the reaction, and k_2 is the rate constant of the second step of the reaction. The time for the reaction is given by t.[27]

The experimental data were fit at long times using equation (8) to find k_2. This assumes that all the reactant has turned into intermediate for these long times. To obtain k_2, the latter exponential part of the curve was fit to the model using equation (8) after 100 minutes.

$$Abs_T = Abs_I + Abs_P$$

$$Abs_T = C\,(1-e^{(-k_2t)}) + E\,e^{(-k_2t)}. \quad (8)$$

3.2.1 Imidazolium *trans*-tetrachloro bis (imidazole) ruthenate(III) Complex (RIM)

The normal absorbance spectra of RIM, illustrated in Figure 9, display two distinct maxima at 340 nm and 400 nm. These two peaks are always observed during the study in all

buffer solutions of different pH values. During hydrolysis, the increase over time for absorption at 340 nm is greater than the increase at 400 nm in every trial as shown in Figure 10. Due to a greater increase in absorption at 340 nm, this wavelength was used for the kinetic analysis of hydrolysis of this complex.

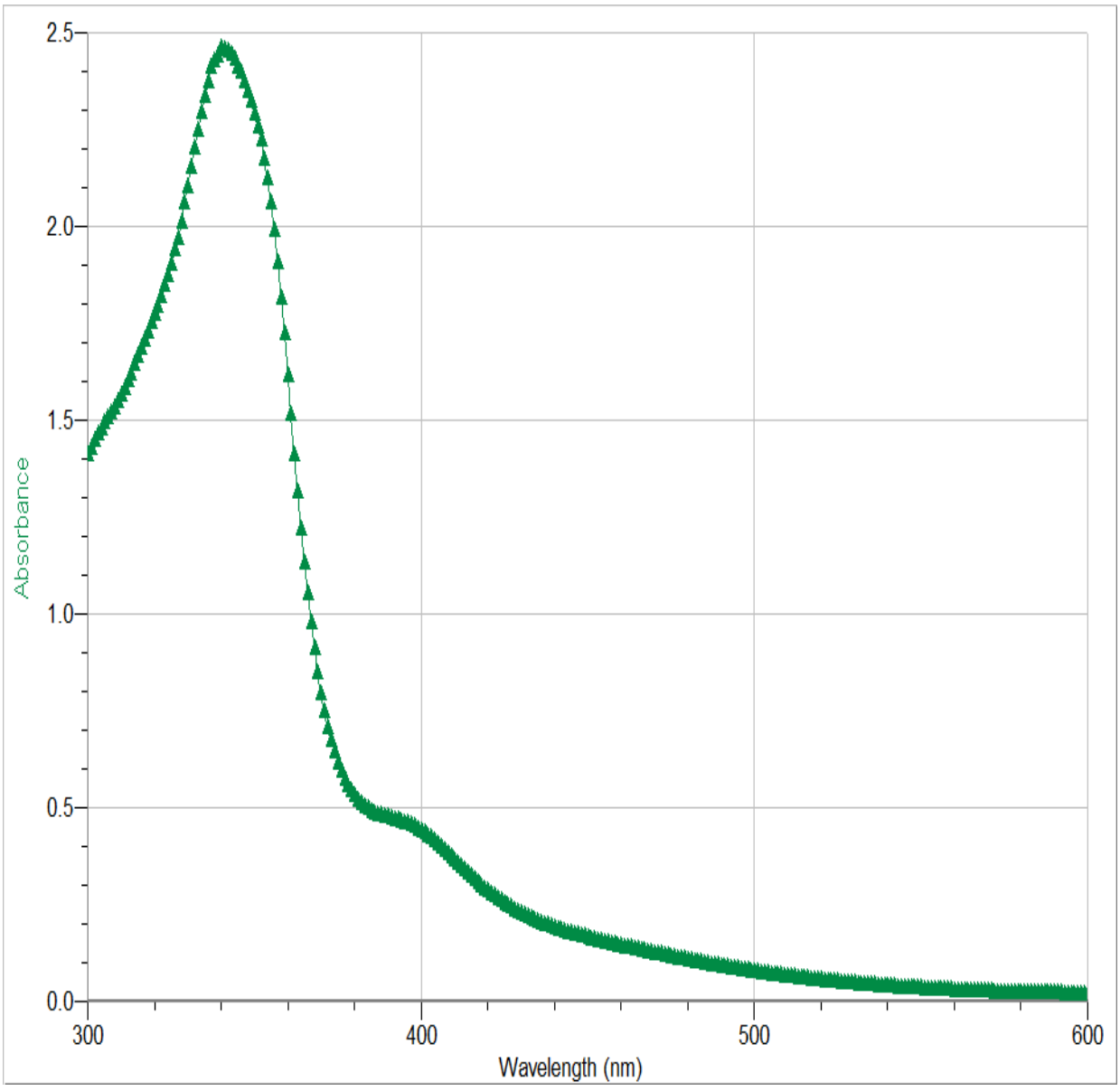

Figure 9. The normal absorbance spectrum of RIM at a pH of 6.0. Two absorbance maxima at 340 nm and 400 nm are observed.

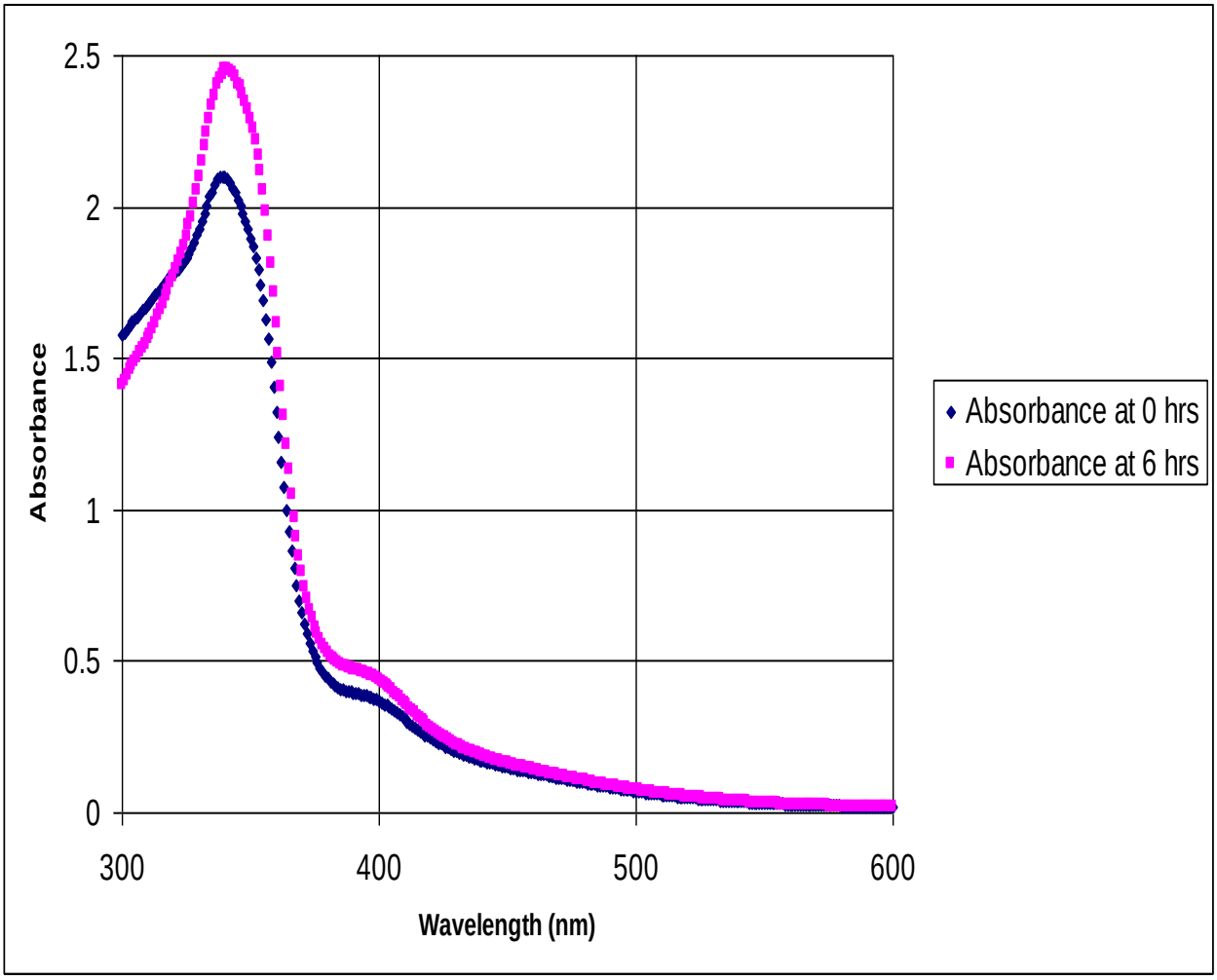

Figure 10. Absorbance spectrum of RIM at a pH of 6.0 over time.

Figure 10 indicates an increase in the absorbance of the RIM complex at 340 nm and 400 nm with time. It clearly indicates that the increase in absorbance at 340 nm is higher than the increase in absorbance at 400 nm.

Based upon the observed absorbance spectra, hydrolysis studies on the RIM complex were conducted at 340 nm at pH values varying from 4.0 to 9.0. The graphs in Figure 11 through Figure 14 show how absorbance of the RIM complex at 340 nm at pH values of 4.0, 5.0, 7.5, and 9.0 changes over time.

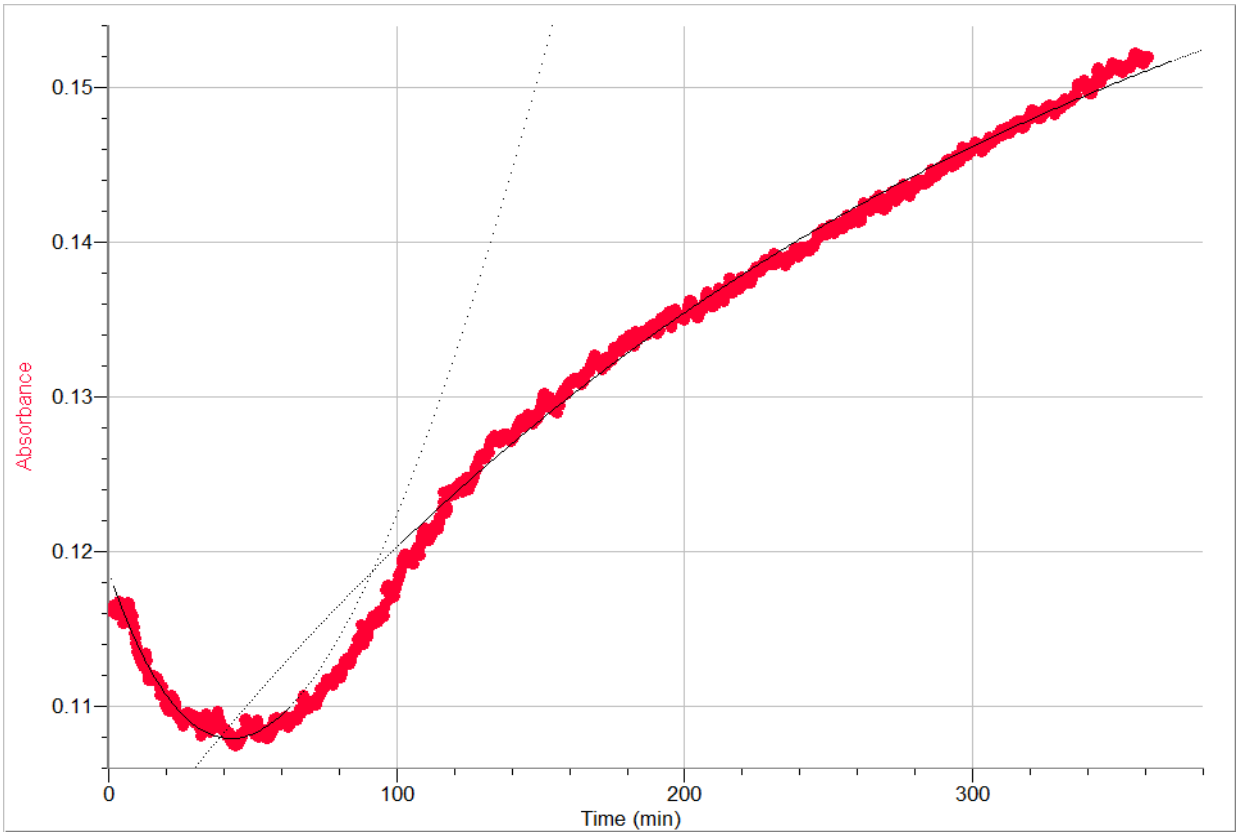

Figure 11. The absorbance of RIM complex monitored at 340 nm at a pH of 4.0 for 6 hours. Equation (7) was used for the best fit on curve before 100 minutes and best fit of of the curve after 100 minutes was obtained by using equation (8).

Figure 11 reveals an initial induction period of 120 minutes during which the intermediate is formed. After the induction period, the rate is governed by the second step, the formation of product from the intermediate. Equation (8) was used to fit the curve after 120 minutes and k_2 was determined. The rate constant k_1 was then determined using equation (7), which gives the best fit for first part of the curve. The average rate constant for a pH of 4.0 for the first step (k_1) was 0.02881 sec^{-1}, and the rate constant of the second step (k_2) was 0.003510 sec^{-1}. It should be noted that the absorbance was measured a day later, was monitored for a few hours, and was found to be constant indicating that the reaction had reached completion.

Though the previous kinetics models proposed were used in determining rate constants, another possible mechanism known as crystal growth may better explain the slower induction period and rapid increase in absorbance in Figure 11, as proposed by Dr. Larry Kolopajlo.[29] The absorbance increase could be due to the increased turbidity in the solution over time. The turbidity is caused by the precipitation of polynuclear complexes in the solution. Further studies must be done in order to confirm whether the precipitate consists of crystals of polynuclear complexes. The first step of crystal growth is nucleation, which is known to be brief. The second step of crystal growth is rapid and evidenced by the increase in turbidity, resulting in a sharp absorbance increase. The crystal growth mechanism seems suitable for all the complexes showing an induction period followed by a rapid increase in absorbance.

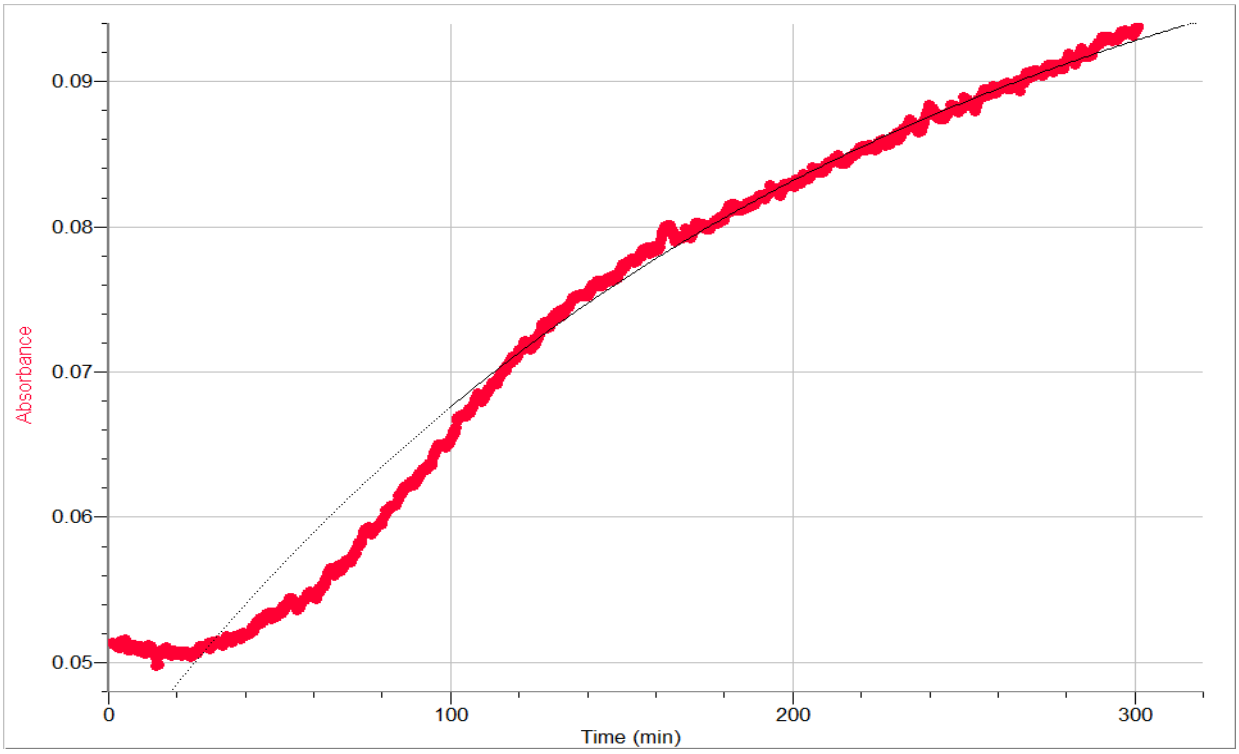

Figure 12. The absorbance of RIM complex monitored at 340 nm at a pH of 5.0 for 5 hours. Equation (8) was used for the best fit on curve after 100 minutes.

Figure 12 clearly indicates that there is an initial induction period of 80 minutes, followed by a sharp increase in absorbance. The average rate constant for k_2 of the data at a pH of 5.0 was 0.004596 sec^{-1} by fitting equation (8) to the curve after 100 minutes. The rate constant (k_1) was 0.02061 sec^{-1}.

The induction period that was clearly observed in graphs at acidic pH levels was found to diminish as pH increased. Figure 13 shows the hydrolysis profile of RIM complex in a buffer solution of pH 7.5. At this pH level, the time taken for nucleation reduces to less than an hour.

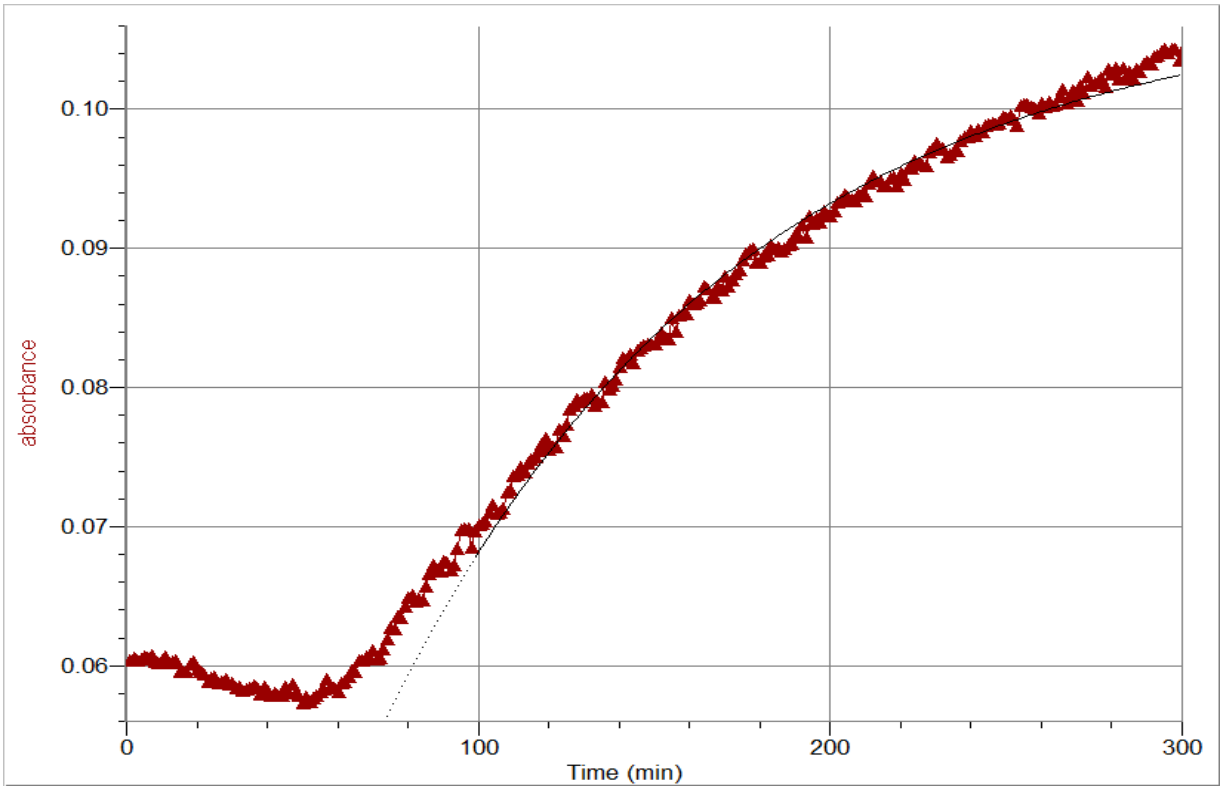

Figure 13. The absorbance of RIM complex monitored at 340 nm at a pH of 7.5 for 5 hours. Equation (8) was used for the best fit on curve after 100 minutes.

The average rate constant for k_2 at pH 7.5 was 0.006331 sec^{-1}, and the rate constant (k_1) was determined to be 0.04145 sec^{-1}.

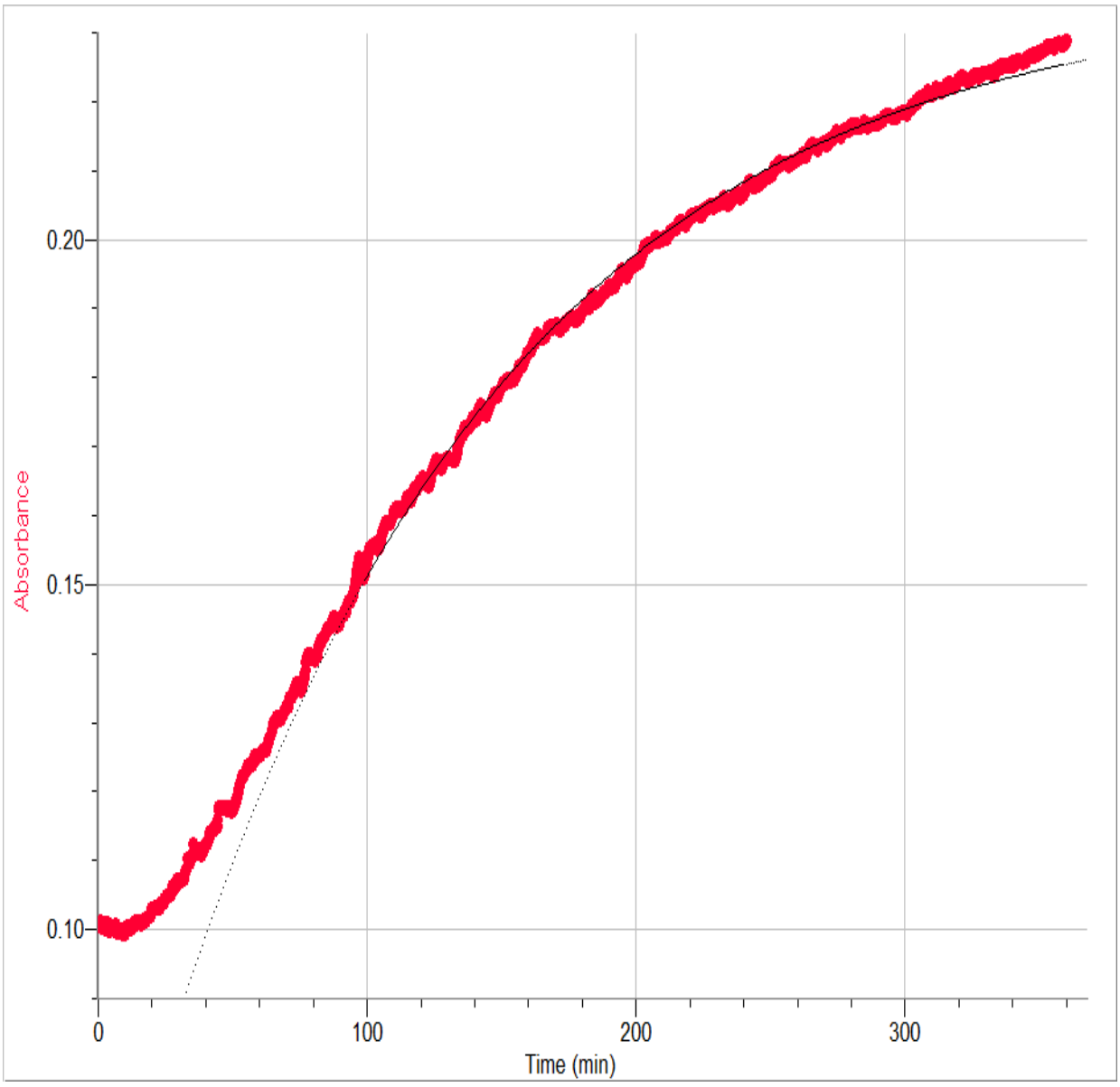

Figure 14. The absorbance of the RIM complex monitored at 340 nm at a pH of 9.0 for 6 hours. Equation (8) was used for the best fit on curve after 100 minutes.

At a pH of 9.0, the induction period was observed to shorten to 20 minutes as shown in Figure 14. This is consistent with a faster formation of the intermediate at higher pH levels. The average rate constant k_2 at this pH was 0.006693 sec^{-1}, and the rate constant k_1 was 0.04289 sec^{-1}.

The rate constants of the two steps of hydrolysis are shown in Table 1. Based upon the results obtained, it can be hypothesized that the hydrolysis of RIM is a two-step process, and the rate of the first step increases at basic pH levels as evidenced by an increase the in value of k_1.

Table 1. Average rate constants for two steps (k_1= first step, k_2 = second step) of hydrolysis of 0.050 M RIM complex at different pH values:

pH	k_1 for all trials (s^{-1})		Average k_1 (s^{-1})	k_2 for all trials (s^{-1})		Average k_2 (s^{-1})
4.0	Trial 1	0.01065	0.02881	Trial 1	0.003794	0.003510
	Trial 2	0.02650		Trial 2	0.003431	
	Trial 3	0.04973		Trial 3	0.003157	
5.0	Trial 1	0.02358	0.02061	Trial 1	0.004778	0.004596
	Trial 2	0.02071		Trial 2	0.002830	
	Trial 3	0.01754		Trial 3	0.006180	
6.0	Trial 1	0.02101	0.01917	Trial 1	0.005526	0.004544
	Trial 2	0.01734		Trial 2	0.003545	
7.5	Trial 1	0.04515	0.04145	Trial 1	0.005275	0.006331
	Trial 2	0.03743		Trial 2	0.009984	
	Trial 3	0.04176		Trial 3	0.003727	
9.0	Trial 1	0.03163	0.04289	Trial 1	0.007976	0.006693
	Trial 2	0.05462		Trial 2	0.005990	
	Trial 3	0.04342		Trial 3	0.006114	

All these values of rate constants have been verified with the Q-test for statistical analysis. For example, at pH = 4.0, trial 3 has a high value, but according to the Q-test used for identifying statistical outliers, it cannot be discarded because the calculated Q-value for the data is 0.59. To

disregard a point with three trials, the Q must be greater than 0.94. Thus, the data for the trial 3 cannot be discarded.

Table 1 indicates that rate constant of the first step of the reaction tends to decrease from the pH values of 4.0 to 6.0 and then starts to dramatically increase at higher pH levels in the range from pH 7.5 to 9.0. The dramatic increase might be due to the higher reactivity of RIM complex with phosphate buffer in basic pH values, resulting in the formation of a ruthenium phosphate complex.[29]

The rate constant of the second step of the reaction shows a different pattern, increasing steadily from pH 4.0 to 9.0. For all pH levels at room temperature, the rate of the first step was found to be almost 10 times faster than the rate of the second step. At higher pH values, k_1 and k_2 increased dramatically, indicating that the complex might be following a different mechanism at these pH values. It is proposed that at high pH's the complex reacts with the phosphate buffer.[29] The comparison of the rate constant k_2 at different pH values is depicted in Figure 15.

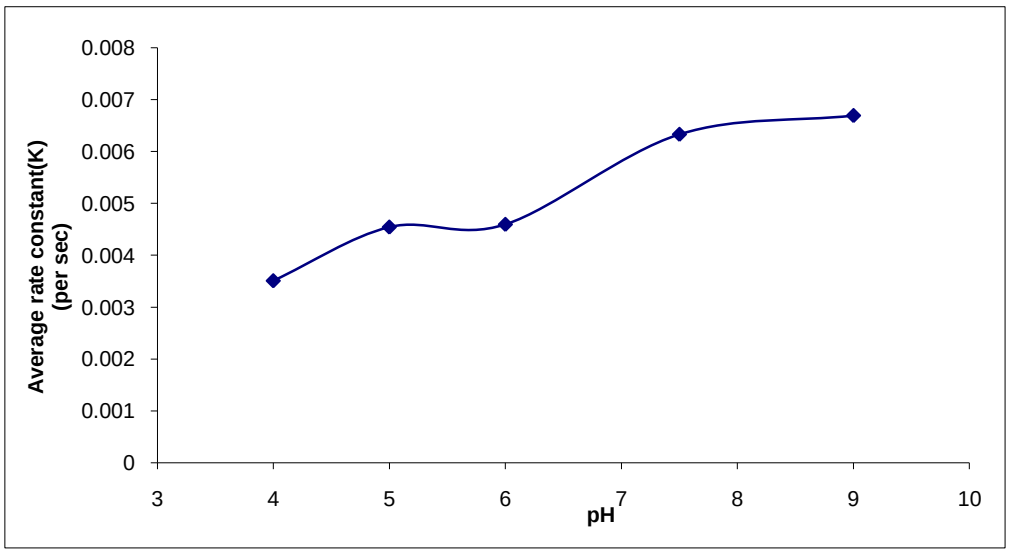

Figure 15. Comparison of k_2 values of the RIM complex at different pH values.

3.2.2 Thiazolium *trans*-tetrachlorobis (thiazole)ruthenate(III) Complex (RTZ)

The absorbance spectra of the RTZ complex showed in Figure 16 displays two absorbance maxima at 365 nm and 420 nm.

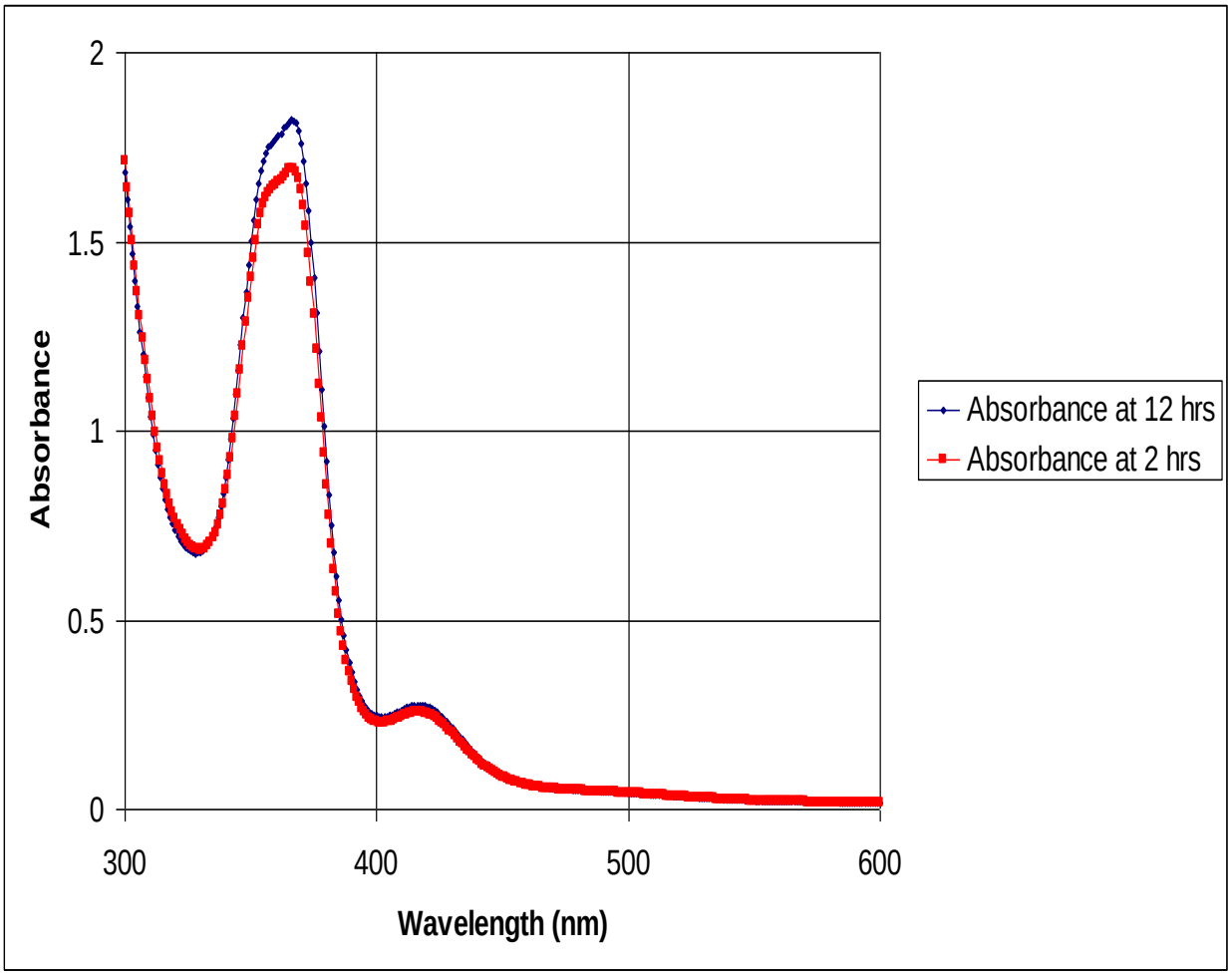

Figure 16. Absorbance spectrum of RTZ complex at a pH of 6.0 over time.

The absorbance spectrum of RTZ complex dissolved in pH 6.0 buffer, shown in Figure 16, clearly indicates a change in the absorbance over time at 365 nm, while the absorbance at 420 nm remains constant. Hence, the study of kinetics of the hydrolysis of RTZ complex was conducted at 365 nm.

Using the wavelength of 365 nm, the kinetics of the RTZ complex was analyzed at various pH values. The graphs in Figures 17 through 20 show the absorbance change of the RTZ complex in buffer solutions of pH of 5.0, 6.0, 7.5, and 9.0 during the time of the reaction.

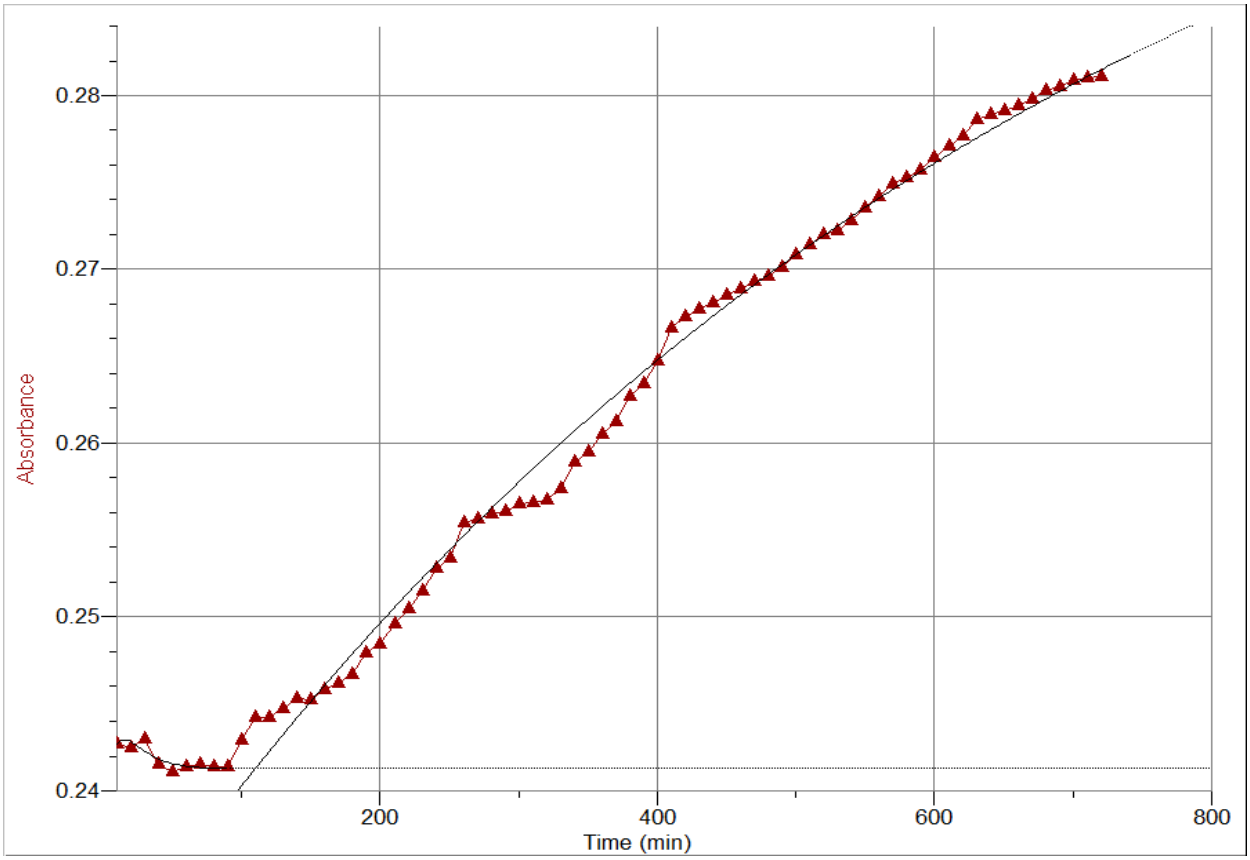

Figure 17. Absorbance of RTZ complex monitored at 365 nm at a pH of 5.0 for 12 hours. Equation (7) was used for the best fit curve before 100 minutes. The best fit of the curve after 100 minutes was obtained by using equation (8).

In Figure 17, an induction period of 100 minutes is observed to fully form the intermediate, followed by the second step of the hydrolysis reaction. The average rate constant of the first step, corresponding to the induction period, was 0.03403 s^{-1}, and average rate constant of the second step, corresponding to the curve at longer times, was found to be 0.003601 s^{-1}.

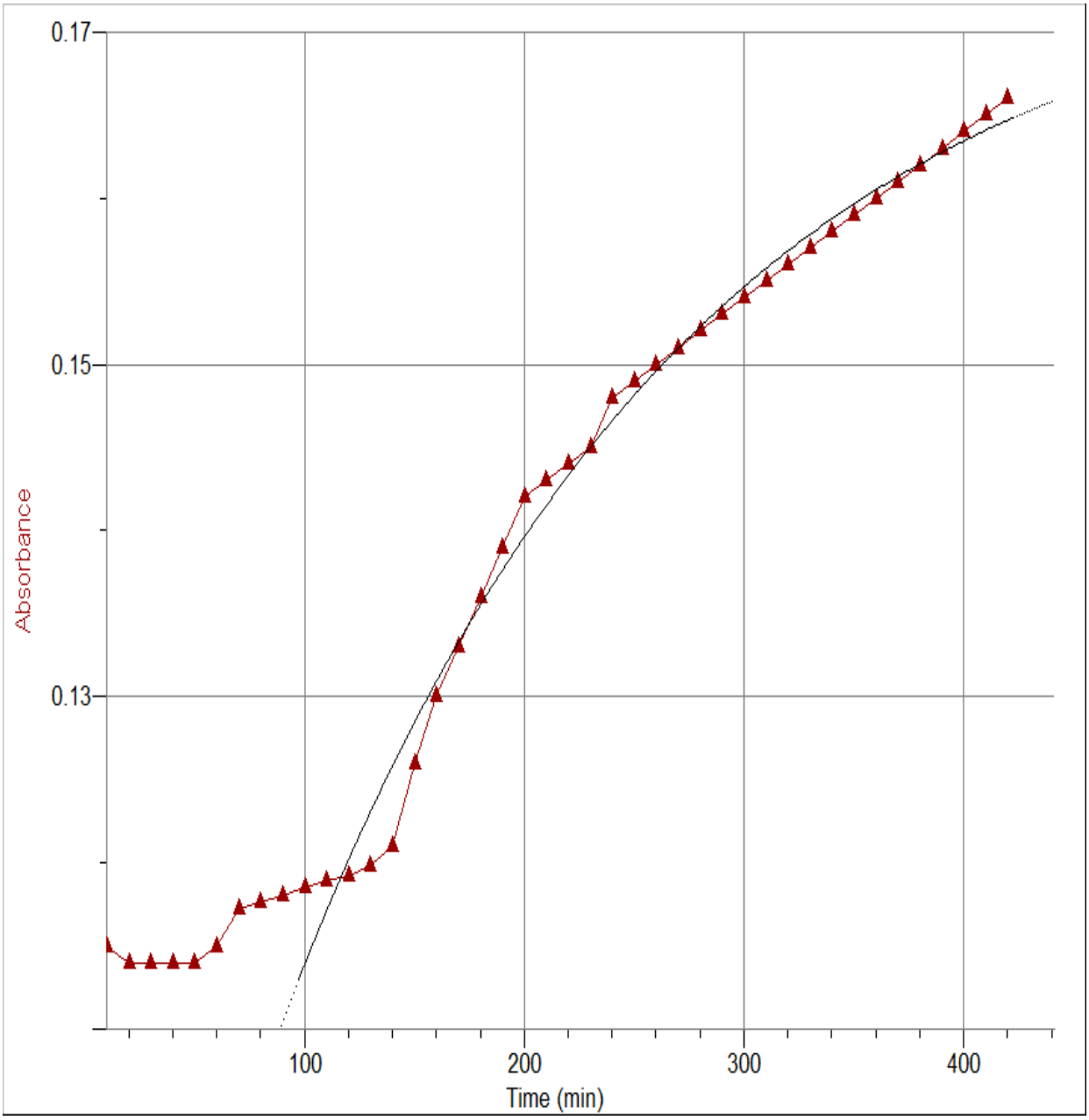

Figure 18. Absorbance of RTZ complex monitored at 365 nm at a pH of 6.0 for 7 hours. Equation (8) was used for the best fit curve after 100 minutes.

In Figure 18, the induction period was observed for a longer time of about 130 minutes and followed by the production of product. The average rate constant for k_2 was 0.006053 s^{-1}. The average rate constant for k_1 was 0.02391 sec^{-1}.

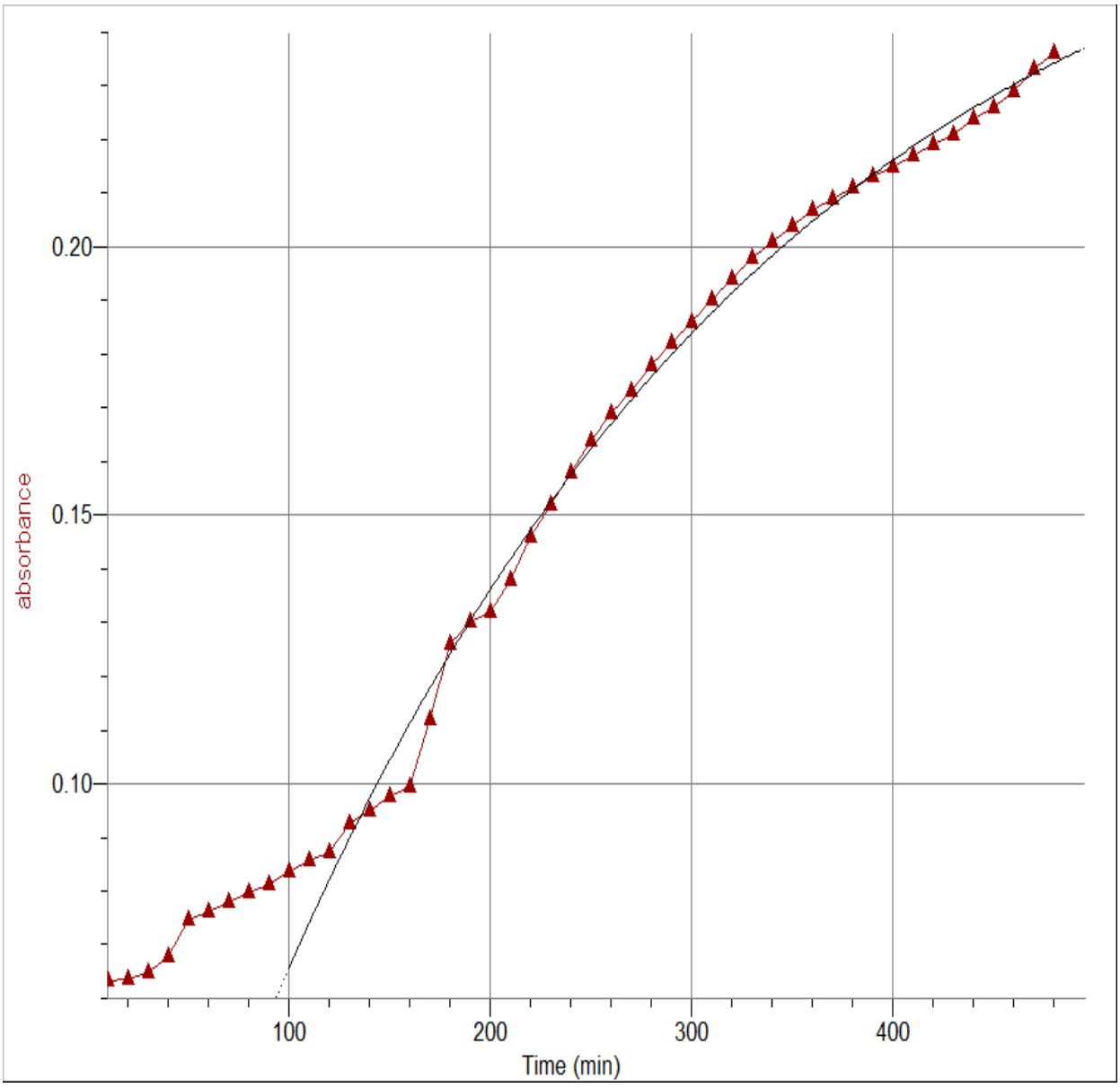

Figure 19. The absorbance of RTZ complex monitored at 365 nm at a pH of 7.5 for 8 hours. Equation (8) was used for the best fit curve after 100 minutes.

The decrease in the induction period is clearly observed in the absorbance spectrum of the RTZ complex at a pH of 7.5, as shown in Figure 19. The rate of hydrolysis increased and was higher at pH 7.5 than at lower pH values. The average rate constant k_2 was 0.006641 sec^{-1}, and k_1 was 0.0443 sec^{-1}.

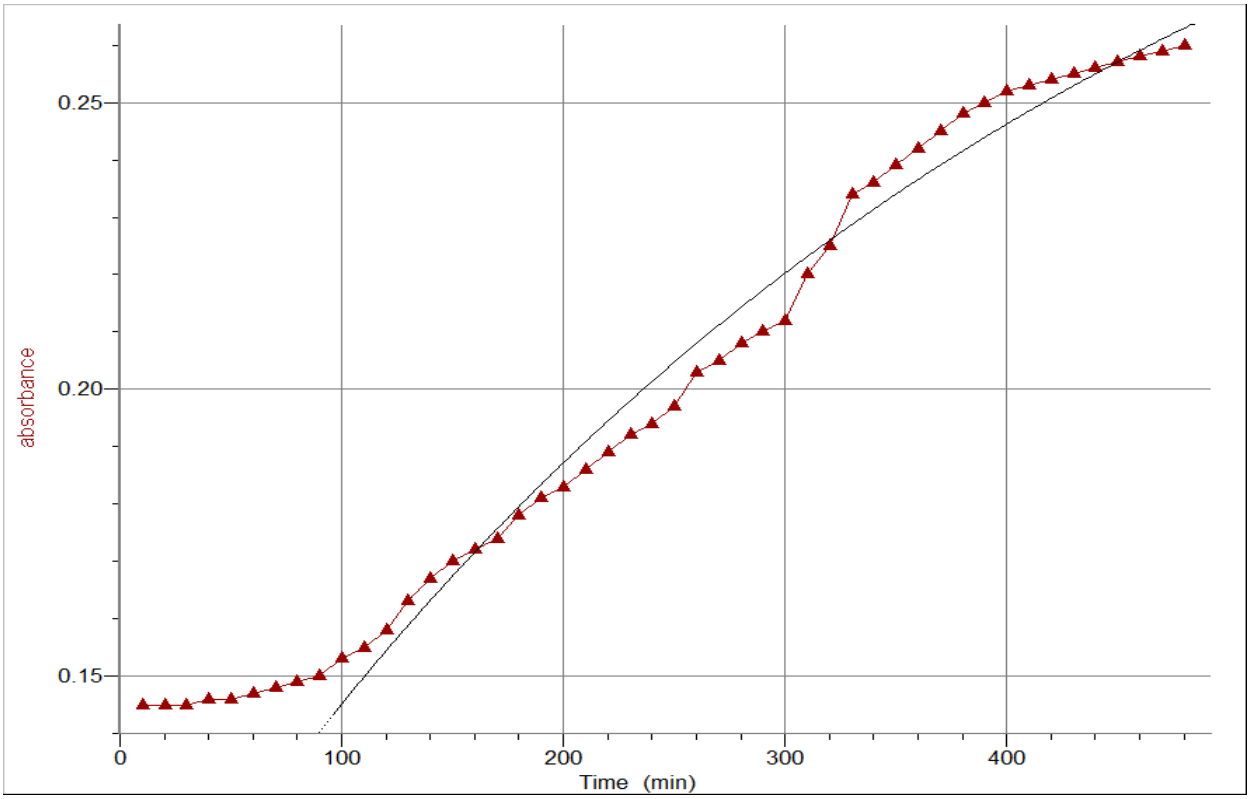

Figure 20. Absorbance of RTZ complex monitored at 365 nm at a pH of 9.0 for 8 hours. Equation (8) was used for the best fit curve after 100 minutes.

In Figure 20 the rate of product formation at a pH of 9.0 appears to increase, and the induction period appears to be shorter than at lower pH's. The average rate constant k_2 was 0.003858 sec^{-1}, and the rate constant k_1 was 0.0459 sec^{-1}.

The induction period for RTZ can also be related to the nucleation of the crystal and the increase in the absorbance of the solution due to the precipitation caused by crystal growth. This hydrolysis mechanism is similar to the kinetics of RIM complex, which may also exhibit the crystal growth mechanism.[29] In basic medium, hydrolysis was anticipated to follow a different mechanism forming a ruthenium phosphate complex indicated by a dramatic change in the rate constant values.

All data were fit using equations (7) and (8) using the Graphical Analysis software. The rate constants at various pH values for the hydrolysis of RTZ complex are displayed in Table 2.

Table 2. Average rate constants for two steps of hydrolysis of 0.045 M RTZ complex at room temperature.

pH	k_1 of all runs (s^{-1})	Average k_1 (s^{-1})	k_2 of all runs (s^{-1})	Average k_2 (s^{-1})
4.0	0.0415	0.03463	0.003192	0.003281
	0.0182		0.003282	
	0.0442		0.003364	
5.0	0.0241	0.03403	0.004062	0.003601
	0.0484		0.001444	
	0.0327		0.005281	
6.0	0.0267	0.02391	0.005385	0.006053
	0.0218		0.006602	
	0.0231		0.006172	
7.5	0.0343	0.0443	0.004007	0.006641
	0.0475		0.008431	
	0.0511		0.007484	
9.0	0.0482	0.0459	0.002408	0.003858
	0.0525		0.005714	
	0.0372		0.003812	

Table 2 clearly indicates that the rate of the hydrolysis of RTZ complex, which is determined by k_2, is highest in a pH 7.5 buffer solution. The rate constant of the first step of the reaction k_1 appeared to decrease from pH values of 4.0 to 6.0 but increased from pH values of 7.5 to 9.0. The rate constant of the second step k_2 appeared to increase constantly from pH 4.0 to 7.5 and then decreased at a pH value of 9.0, which might be due to the interaction of the RTZ complex with phosphate buffer at higher pH values.[29] The values of k_2 at different pH values are illustrated in Figure 21.

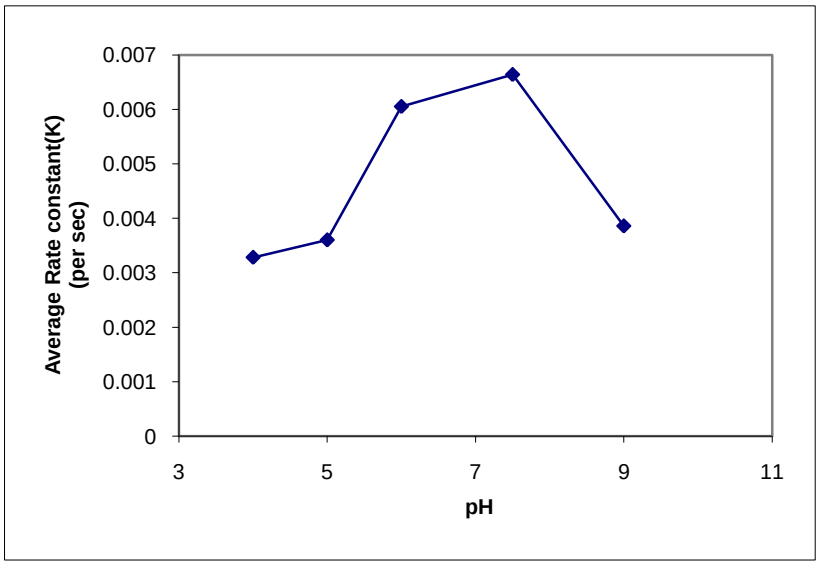

Figure 21. Comparison of rate constant k_2 values of RTZ complex at various pH values.

3.3 1H-1,2,4-triazolium *trans*-tetrachlorobis (triazole) ruthenate(III) Complex (RTrz)

The absorbance spectra of the RTrz complex, shown in Figure 22, displays two absorbance maxima, at 360 nm and at 420 nm. The peak at 420 nm remains constant over time, but the peak at 360 nm shows a significant decrease of absorbance over time. Thus, the peak at 360 nm was utilized for studying the hydrolysis profiles of the RTrz complex.

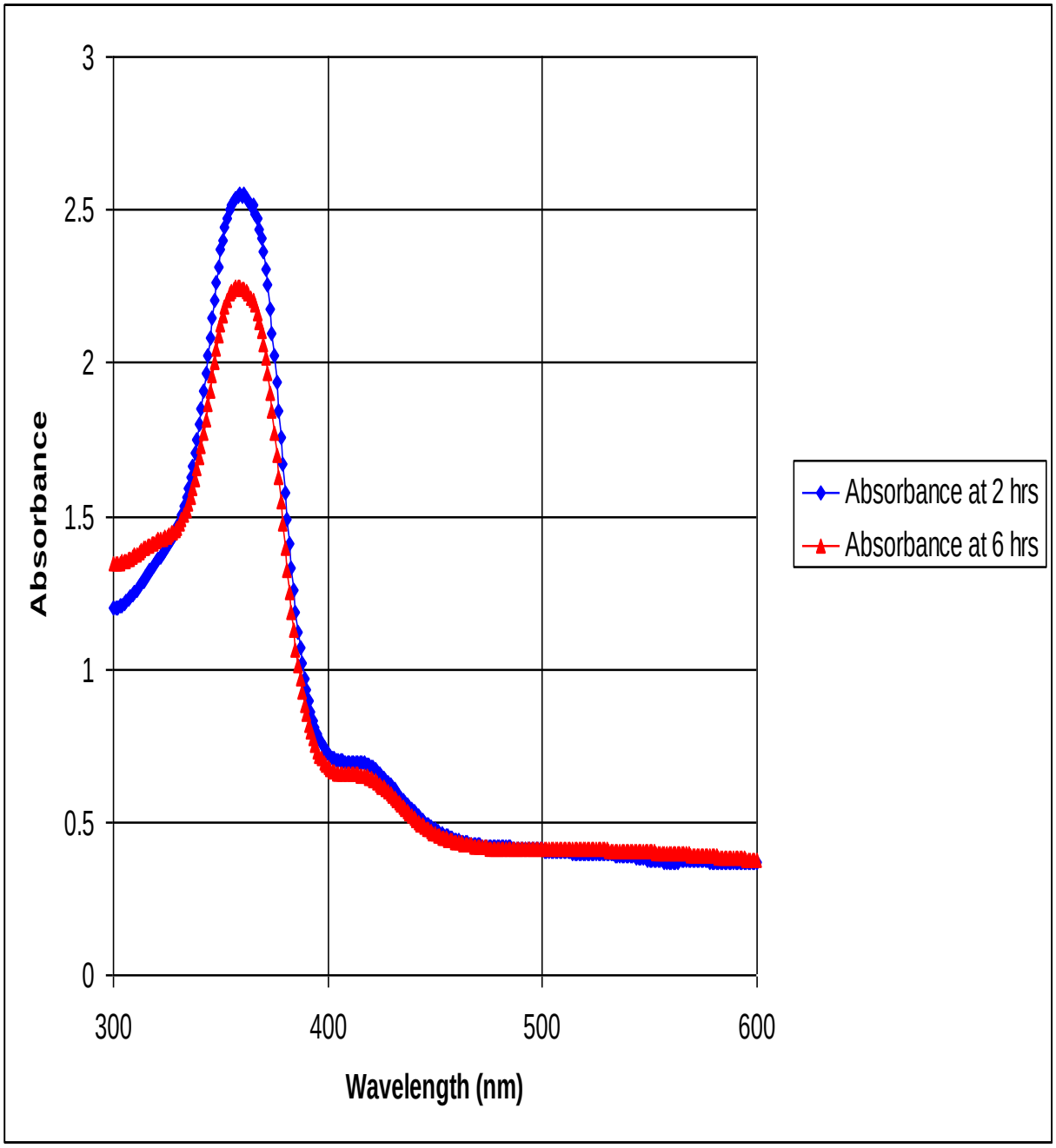

Figure 22. Absorbance profile of RTrz complex at a pH of 6.0 over time.

Hydrolysis studies of the RTrz complex were conducted at different pH levels over time by observing the changes in absorbance at 360 nm. Figures 23 through 25 display absorbance profiles of RTrz complex over time at pH levels of 4.0, 6.0, and 9.0.

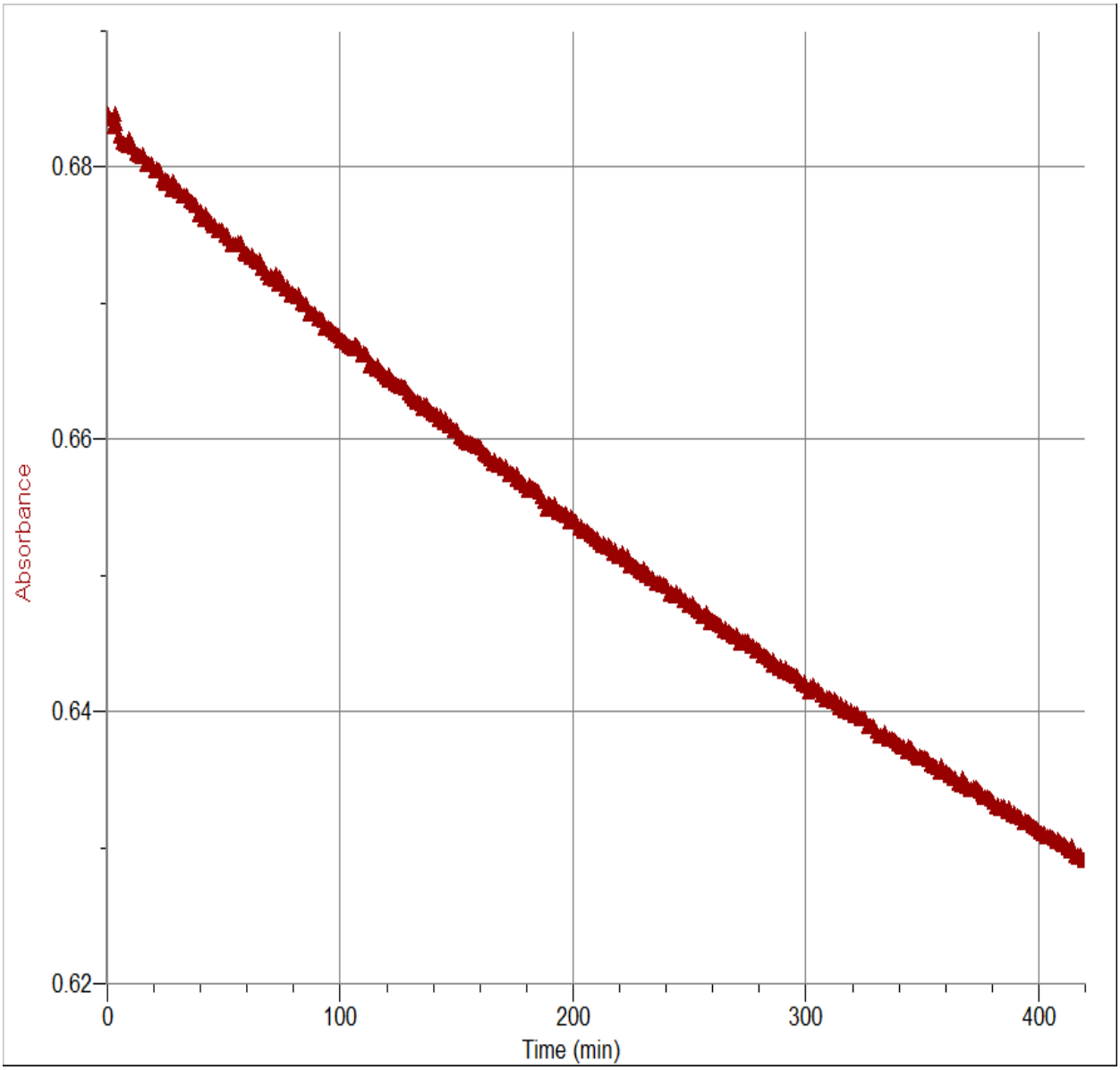

Figure 23. Absorbance of RTrz complex monitored at 360 nm at a pH of 4.0 for 7 hours

The curve in Figure 23 shows the rate of hydrolysis for RTrz complex at a pH of 4.0. All the equations used for attaining the best fit for the curves obtained for the RIM, RTZ complexes were utilized to fit the RTrz kinetic curve, but none gave an appropriate fit. Hence it was hypothesized that the RTrz complex follows a different hydrolysis mechanism, and further studies must be done to properly model the kinetics of the reaction.

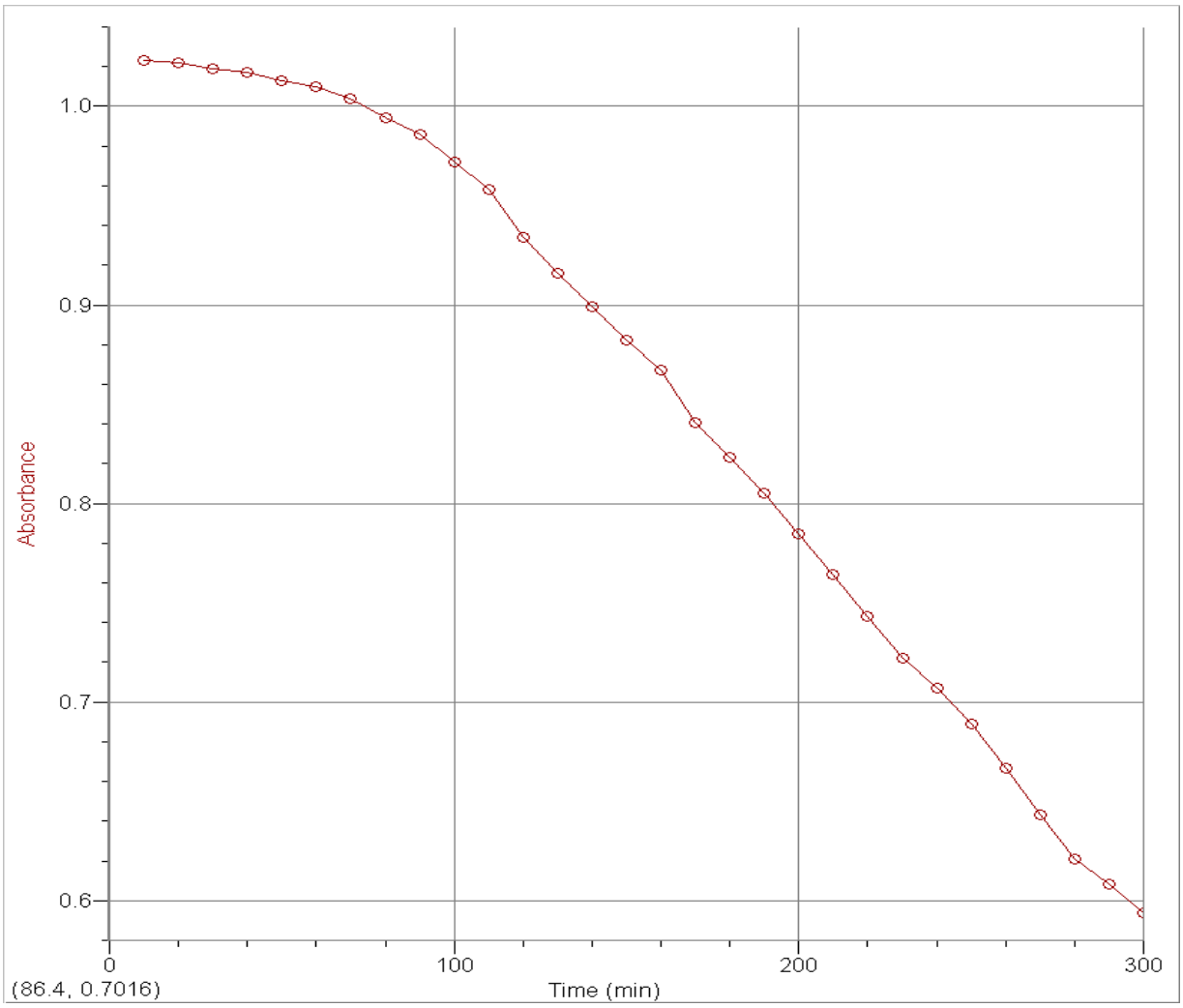

Figure 24. Absorbance of RTrz complex monitored at 360 nm at a pH of 6.0 for 5 hours.

The curve in Figure 24 displays a flat portion for times less than 75 minutes for the hydrolysis of the RTrz complex in a pH of 6.0 buffer solution. After 75 minutes, the absorbance displays a dramatic decrease. In acidic media, the solution was hazy but cleared within minutes, resulting in a decrease in absorbance. The hydrolysis trend of RTrz complexes in acidic media followed the opposite trend in absorbance than the other studied complexes in acidic pH. The RTrz complex displayed a decrease in absorbance during hydrolysis, while the other complexes exhibited an increase in absorbance.

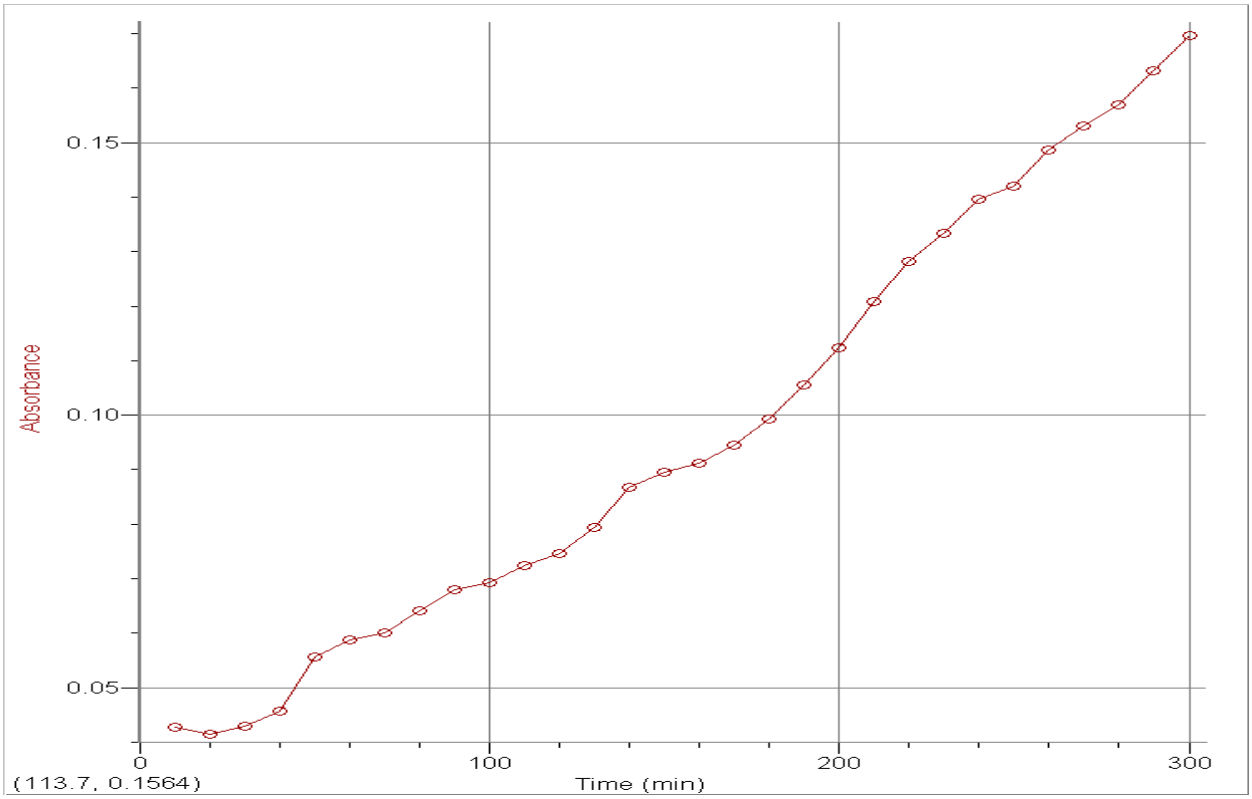

Figure 25. Absorbance of RTrz complex monitored at 360 nm at a pH of 9.0 for 5 hours.

Figure 25 shows the hydrolysis profile of the RTrz complex at a pH of 9.0. This curve shows an increase in absorbance with time, which seems to indicate that a different species is produced in basic solutions than acidic solutions. Initially, the solution was clear but became turbid over time; this indicated the sensitivity of the RTrz complexes to pH conditions.

No kinetic rate constants were derived because proposed models based upon the differential equations for the calculation of rate constants did not fit the data. The species produced in the hydrolysis of the RTrz complex seem to be very sensitive to pH, showing dramatically different patterns of absorbance at different pH values. Hence, to explain this complexity, further studies should be done to understand the nucleation (induction period) and crystal growth (increase or decrease of absorbance) steps.

CHAPTER 4: CONCLUSIONS

The ruthenium complexes studied in this research exhibited different rates of hydrolysis for formation of product as shown in Table 3. No data analysis was performed for RTrz because no known model could fit the data.

In both the RIM and RTZ complexes, hydrolysis profiles show an induction period within approximately the first 100 minutes. After the induction period, an increase in the hydrolysis rate was observed in almost all solutions, regardless of the pH. The rate constant, k_2, increases as pH increases from 4.0 to 7.5 and then either decreases or shows a slight increase from pH 7.5 to 9.0 for all complexes in this study.

The mechanism of hydrolysis for the RTrz complex was different from the mechanism exhibited by other complexes. The absorption curves changed dramatically at basic pH's, implying that a new species was formed in this reaction compared to that formed under acidic conditions. The complex exhibits different hydrolysis patterns in acidic and basic solutions, indicating that the species produced during the hydrolysis of the RTrz complex is dependent on pH. Further studies such as NMR and LC-MS could help in resolving the kinetics of the RTrz hydrolysis.

The increase or decrease in absorbance for these complexes was due to the increase or decrease in turbidity in the solution. This turbidity was attributed to the precipitation occurring in the solution. The mechanism for the precipitation reflects the crystal growth mechanism which includes two phases. The first step is the nucleation, and the second step is the growth of the crystal. Further studies must be conducted in order to elucidate the structure of the crystals formed and elucidate the two steps more clearly.

Table 3. Comparison of rate constants (k_2) of the hydrolysis of RIM and RTZ complexes at different pH values

	Rate constant (k_2) in pH 4.0 (sec^{-1})	Rate constant (k_2) in pH 5.0 (sec^{-1})	Rate constant (k_2) in pH 6.0 (sec^{-1})	Rate constant (k_2) in pH 7.5 (sec^{-1})	Rate constant (k_2) in pH 9.0 (sec^{-1})
RIM complex	0.003510	0.004596	0.004544	0.006331	0.006693
RTZ complex	0.003281	0.003601	0.006053	0.006641	0.003858

The rate constant, k_2, for the hydrolysis of the RIM complex was found to be higher for higher pH levels. The hydrolysis of the RTZ complex was found to be highest in pH 7.5 buffer. Hence these two complexes can be considered as good choice for controlling the rapid growing cells in initial stages of cancer as the rate of active drug formation will be high at pH 7.5, which is close to the pH of the blood stream, 7.4.[19]

The RTrz complex exhibited a rapid decrease in absorbance in higher pH levels, indicating the possibility of rapid hydrolysis. The increase or decrease in absorbance correlates to the pace of the hydrolysis reaction of the complexes, and the faster hydrolysis reaction indicates faster decomposition of the Ru (III) form. Hence, it indicates the shelf life of this complex is highly dependent upon the pH of the environment to which this complex is being exposed.

The higher the basicity of an azole ligand, the higher will be the energy of its excited state and the more stable will be the Ru (III) state. All these factors affect the rate of hydrolysis.[22,25] The increasing order of the basicity of the ligands in this study is as follows:

Triazole (pK_a =2.2) < Thiazole (pK_a =3.5) < Imidazole (pK_a =6.99).[22]

Because imidazole and thiazole are more basic, they have more electron donor character than the triazole ligand. As the basicity of the ligand increases, the active form of ruthenium [Ru (II)] becomes destabilized, thus requiring more time for its inactive form [Ru (III)] to be reduced.[22, 25] Thus, the mechanism of hydrolysis is dependent on the basicity of the ligands complexed with the metal. More in-depth studies need to be done to characterize the steps of hydrolysis more clearly.

Future Aspects:

A background spectrum of the phosphate buffer and a spectrum of the individual ligands, and a comparison of these spectrums with that of the complexes, will be helpful in elucidating the kinetics and behavior of these complexes at various pH values.

The hydrolysis studies, conducted at different temperatures and in different solvents, may affect the stability of ruthenium complexes. NMR spectroscopy and HPLC –MS may be utilized in the analysis of the hydrolysis in order to reveal the exact chemical structures of the intermediate and product formed during the hydrolysis reactions. This study can be extended to similar ligands like pyrazole, pyrimidine, phenanthrolines, and their derivatives in order to further understand the effect of basicity of these ligands on the hydrolysis of these ruthenium complexes. A future kinetic study of the ruthenium complexes bound to various purine and pyrimidine bases of DNA at various pH levels may reveal important pharmacological parameters such as the rate of drug release, the onset of action, and the duration of action of these complexes. These results may help in better designing these complexes in the future.

REFERENCES

1. Kostova, I. Ruthenium Complexes as Anticancer Agents. *Curr. Med. Chem.* **2006,** *13*, 1085-1107.
2. Kratz, F.; Hartmann, M.; Keppler, B.; Messori, L. The Binding Properties of Two Antitumor Ruthenium (III) Complexes to Apotransferrin. *J. Bio. Chem.* **1994,** *4*, 2581-2588.
3. Piccioli, F.; Sabatani, S.; Messori, L.; Orioli, P.; Hartinger, C. G.; Keppler, B. K. A Comparative Study of Adduct Formation Between the Anticancer Ruthenium (III) Compound HInd trans-[$RuCl_4(Ind)_2$] and Serum Proteins. *J. Inorg. Biochem.* **2004**, *98*, 1135-1142.
4. Rubin, R.; Strayer, S. D. Rubin's Pathology-Clinicopathologic Foundations of Medicine. 5th edition, A Lippincott Williams and Wilkins, **2007,** 152.
5. http://www.biologydaily.com/biology/Cancer, 10/05/09, 2.00 pm.
6. Kozelka, J.; Legendre, F.; Reeder, F.; Chottard, J. C. Kinetic Aspects of Interactions between DNA and Platinum Complexes. *Co. Chem. Rev.* **1999,** *190-192*, 61-82.
7. Pramod, K. Kinetic studies of the hydrolysis reactions of ruthenium (III) complexes Him trans-[$RuCl_4(im)_2$] and Hind trans-[$RuCl_4(ind)_2$] by UV-Visible spectrophotometry. *Eastern Michigan University Chemistry Department Thesis* **2007**.
8. Fichtinger-Schepman, A.; Lohman, P. H.; Reedijk, J. Detection and Quantification of Adducts Formed upon Interaction of Diamminedichloroplatinum (II) with DNA by Anion-Exchange Chromatography After Enzymatic Degradation. *Nuc. Ac. Res.* ***1982,*** *10*, 5345-5356.

9. Eastman, A. Reevaluation of Interaction of Cis-dichloro(ethylenediamine)platinum (II) with DNA. *Biochemistry* **1986,** *25*, 3912-3915.

10. Lohman, P.H.; Reedijk, J. Fichtunger-Schepman, A. M.; Van der Veer, J. L.; Den hartog, J. H. Adducts of the Antitumor Drug Cis-diamminedichloroplatinum (II), with DNA: Formation, Identification, and Quantitation. *Biochemistry* **1985,** *24*, 707-713.

11. Siddik, Z.; Cisplatin: Mode of Cytotoxic Action and Molecular Basis of Resistance. *Oncogene* **2003,** 22, 7265-7279.

12. Brabec, V.; Novakova, O. DNA Binding Mode of Ruthenium Complexes and Relationship to Tumor Cell Toxicity. *Drug Resistance Updates* **2006,** *9*, 111-122.

13. Zeller, W. J.; Fruehauf, D. New Platinum, Titanium, and Ruthenium Complexes with Different Patterns of DNA Damage in Rat Ovarian Tumor Cells. *Cancer Research* **1991,** *51*, 2943-2948.

14. Novakova, O.; Kasparkova, J.; Vrana, O.; Van Vliet, P. M.; Reedijk, J.; Brabec, V. Correlation Between Cytotoxicity and DNA Binding of Polypyridyl Ruthenium Complexes. *Biochemistry* **1995,** *34*, 12369-12378.

15. Chatlas, J.; Eldik, R. V.; Keppler, B. K. Spontaneous Aquation Reactions of a Promising Tumor Inhibitor Trans-imidazolium- tetrachlorobis(imidazole) Ruthenium (III), Trans-Him[RuCl4$(Im)_2$]. *Inorg. Chim Acta*. **1995,** 233, 59-63.

16. Bouma, M.; Nuijen, B.; Jansen, M. T.; Sava, G.; Bult, A.; Beijnen, J. H. Photostability Profiles of the Experimental Antimetastatic Ruthenium Complex NAMI-A. *J. of Pharm. And Biomed. Anal.* **2002,** *30*, 1287-1296.

17. Bacac, M.; Hotze, A. C. G.; Schilden, K.; Haasnoot, J. G.; Pacor, S.; Alessio, E.; Sava, G.; Reedijk, J. The Hydrolysis of the Anti-cancer Ruthenium complex NAMI-A affects

its DNA Binding and Antimetastatic Activity: an NMR evaluation. *J. of Inorg. Biochem.* **2004,** *98*, 402-412.

18. Velders, A. H.; Bergamo, A.; Alessio, E. Synthesis and Chemical−Pharmacological Characterization of the Antimetastatic NAMI-A-Type Ru(III) Complexes (Hdmtp)[*trans*-$RuCl_4$(dmso-S)(dmtp)], (Na)[*trans*-$RuCl_4$(dmso-S)(dmtp)], and [*mer*-$RuCl_3(H_2O)$(dmso-S)(dmtp)] (dmtp = 5,7-Dimethyl[1,2,4]triazolo[1,5-*a*]pyrimidine). *J. Med. Chem.* **2004,** 47(5), 1110-1121.
19. Mura, P.; Camalli, M.; Messori, L.; Piccioli, F.; Zanello, P.; Corsini, M. Synthesis, Structural Characterization , Solution Chemistry, and Preliminary Biological Studies of the Ruthenium (III) Complexes [TzH][trans-$RuCl_4(Tz)_2$] and [TzH][trans-RuCl4(DMSO)(Tz)].(DMSO), the Thiazole Analogues of Antitumor ICR and NAMI-A. *Inorg. Chem.* **2004,** *43*, 3863-3870.
20. Mura, P.; Messori, L.; Camalli, M. Structure- Function Relationships within Keppler – Type Antitumor Ruthenium (III) Compelxes: the Case of 2- Aminothiazolium[*trans*-tetrachlorobis(2-aminothiaole)ruthenate(III)]. *Inorg. Chem.* **2005,** 44, 4897-4899.
21. Iengo, E,; Mestroni, G.; Geremia, S.; Calligaris, M.; Alessio, E. Novel Ruthenium(III) Dimmers Na_2[{trans-$RuCl_4(Me_2SO\text{-}S)\}_2$] and [{mer, cis-$RuCl_3(Me_2SO\text{-}S)(Me_2SO\text{-}O)\}_2$] Closely Related to the Antimetastatic Complex Na[trans-$RuCl_4(Me_2SO\text{-}S)$(Him)]. *Inorg. Chem.* **1999,** *19*, 3361-3371.
22. Reisner, E.; Arion, V.; Guedes da Silva, M.; Fatima, C.; Lichtenecker, R.; Eichinger, A.; Keppler, B. K.; Pombeiro, A. J. L. Tuning of Redox Potentials for the Design of Ruthenium Anticancer Drugs- an Electrochemical Study of [trans-$RuCl_4$L(DMSO)] and

[trans-$RuCl_4L_2$]- Complexes, where L=Imidazole, Indazole,1,2,4-triazole. *Inorg. Chem.* **2004,** *43*, 7083-7093.

23. Skoog, A. D.; Holler, F.J.; Crouch, R.S.; Principles of Instrumental Analysis. 6th edition, A Thomson Brooks/Cole publication, **2007,** 336-362.
24. Keppler, B. K.; Rupp, W.; Juhl, U.M.; Endres, H.; Niebl, R.; Balzer, W. Synthesis, Molecular Structure, and Tumor-Inhibiting Properties of Imidazolium Trans-Bis(imidazole)tetrachlororuthenate (III) and Its Methyl-Substituted Derivatives. *Inorg. Chem.* **1987,** *26*, 4366-4370.
25. Kung, A.; Pieper, T.; Wissiack, R.; Rosenberg, E.; Keppler, K. B. Hydrolysis of the tumor –inhibiting ruthenium(III) complexes HIm trans-[$RuCl_4(im)_2$] and Hind trans-[$RuCl_4(ind)_2$] Investigated by means of HPCE and HPLC-MS. *J. Biol. Inorg. Chem.* **2001,** 6, 292-299.
26. Arion, V.; Reisner, E.; Fremuth, M.; Jakupec, A.M. Synthesis, X-ray Diffraction Structures, Spectroscopic Properties, and in vitro Antitumor Activity of Isomeric (1H-1,2,4- Triazole) Ru(III) Complexes. *Inorg. Chem.* **2003,** 42, 6024 -6031.
27. Atkins, P.; Paula, J. *Physical chemistry, 7th edition,* W.H. Freeman and Company. **2002,** 883-884.
28. Laidler, K. J.; Meiser, J. H.; Sanctuary, C. B.; *Physical Chemistry*, *4th edition*, Houghton Mifflin Company, **2003,** 368-378.
29. Dr. Kolopajlo, Larry. Private communication, 11/02/2010.